

PREPARATION OF ALBUMIN-TARGETED LIPOSOMES AND
THEIR RELEASE CHARACTERISTICS
USING ULTRASOUND

by

Renad Turki

A Thesis Presented to the Faculty of the
American University of Sharjah
College of Engineering
in Partial Fulfillment
of the Requirements
for the Degree of

Master of Science in
Chemical Engineering

Sharjah, United Arab Emirates

January, 2016

Approval Signatures

We, the undersigned, approve the Master's Thesis of Renad Turki

Thesis Title: Preparation of albumin-targeted liposomes and the study of their release characteristics using ultrasound.

Signature

Date of Signature

Dr. Ghaleb Al Hussein
Professor, Department of Chemical Engineering
Thesis Advisor

Dr. Zaroook M. Shareefdeen
Associate Professor, Department of Chemical Engineering
Thesis Committee Member

Dr. Ana Martins
Visiting Scholar, Department of Chemical Engineering
Thesis Committee Member

Dr. Naif Darwish
Head, Department of Chemical Engineering

Dr. Mohamed El-Tarhuni
Associate Dean, College of Engineering

Dr. Leland Blank
Dean, College of Engineering

Dr. Khaled Assaleh
Interim Vice Provost for Research and Graduate Studies

Acknowledgments

First, I would like to express my deep gratitude to my thesis advisor, Dr. Ghaleb Al Hussein, whose passion for the research topic had a lasting effect, and who gave me deep insights throughout the previous semesters. Many thanks, Dr. Ghaleb, for giving me the opportunity of working on this project.

In addition, I would like to thank Dr. Ana Martins and Dr. Rute Vitor for being the greatest mentors who provided me with their valuable suggestions and kindness. I cannot forget to thank my colleagues Salma Ahmed, and Hesham Gamal, for all their help and support while working on my thesis.

Many thanks also go to Dr. Mohammad Al-Sayah for his collaboration in this work and to Dr. Zaroob Shareefdeen for his contribution as thesis committee member. I also want to thank the Department of Chemical Engineering at the American University of Sharjah, for providing me with a teaching assistantship throughout my M.S. studies. Also, I would like to acknowledge the Chemistry Department at the American University of Sharjah for their collaboration.

Last but not least, to the research group members, colleagues, family, friends, and all my beloved ones, thank you all for your continuous support and help to complete my thesis.

Abstract

The main objective of this thesis was to investigate the enhancement of drug delivery using targeted liposomes triggered by ultrasound. In this thesis, a thorough literature review on cancer and drug delivery systems (especially liposomes) was conducted. An overview of nanoparticles as drug delivery carriers, different types of drug targeting and the use of ultrasound to control drug release from nanocarriers is also reported. In the study, albumin-targeted liposomes (proteoliposomes) were prepared and loaded with the model drug calcein. The release studies were performed using different ultrasound power densities at 20-kHz. The size of both liposomes types was determined by Dynamic Light Scattering. The release experiments were done online, by continuously measuring the increase in fluorescence when the calcein self-quenching was relieved upon release. The 20-kHz ultrasound was applied in 20 s pulses with a 10 s inter-pulse interval. In the end, total release was determined by lysing the remaining liposomes with Triton X-100. The prepared liposomes were large unilamellar vesicles with diameters 208.52 ± 11.50 nm (non-targeted control liposomes) and 218.27 ± 12.73 nm (albumin liposomes). Although albumin liposomes are larger, the difference was not significant. For both liposome types, the 20-kHz ultrasound-induced release was fast, reaching a stable value after 150 – 250 s. The release rate increased with increasing power densities, and the final percentage of release was higher than 90% for all power densities. For the same power density, the release from non-targeted liposomes was significantly faster than for albumin liposomes, which suggests that the addition of the albumin moiety changes the acoustic properties of the liposomes, apparently increasing their stability and making them less susceptible to ultrasound. The findings allowed us to conclude that these liposomes could be promising nanocarriers for the anti-cancer drug doxorubicin, enhancing the therapeutic efficacy of the drug and decreasing the side effects of the common chemotherapy cancer treatment.

Search Terms: *Drug delivery systems, prostate cancer, ultrasound-mediated liposomes, PEGylated liposomes, Albumin, Low-Frequency-Ultrasound.*

Table of Contents

Abstract	5
Chapter 1: Introduction	11
Chapter 2: Literature Review	16
2.1. Nanoparticles as Drug Delivery Systems	16
2.1.1. Liposomes.	16
2.1.2. Micelles.	18
2.1.3. Dendrimers.	18
2.1.4. Nanoemulsions.	19
2.1.5. Protein-bound paclitaxel.....	19
2.2. Targeted Drug Delivery Systems.....	19
2.2.1. Passive targeting.....	20
2.2.2. Active targeting.	21
2.2.3. Ultrasound-triggered release from liposomes.....	22
2.3. Relevant <i>in vitro</i> Studies.....	24
2.4. Relevant <i>in vivo</i> Studies.....	25
Chapter 3: Experimental Procedures	27
3.1. Chemicals and Reagents	27
3.2. Methodology.....	27
3.2.1. Preparation of DSPE-PEG-pNP control liposomes.....	27
3.2.2. Preparation of DSPE-PEG-Albumin targeted liposomes.....	29
3.2.3. Determination of the liposome size by dynamic light scattering.	29
3.2.4. Release experiments.....	30
3.2.5. Statistical analysis.	31
Chapter 4: Results and Discussion	32
4.1. Liposome Size	32
4.2. Online Low Frequency US (LFUS)-induced Release	33
4.2.1. Online LFUS-induced release from DSPE-PEG-pNP control liposomes.	34
4.2.2. Online LFUS-induced release from DSPE-PEG-Albumin liposomes..	37

4.2.3. Comparison between US release from targeted micelles and targeted liposomes.....	39
4.2.4. Comparison between control and Albumin-targeted liposomes.	40
Chapter 5: Conclusion and Recommendations.....	44
References	45
Vita	50

List of Figures

Figure 1.1: Schematic of cancer cell abnormal growth [1]	11
Figure 1.2: Schematic representing the structure of liposomes . (a) encapsulating hydrophobic drug; (b) encapsulating hydrophilic drug; (c) modified with ligand or moiety [18]	14
Figure 2.1: Schematic depicting structures and types of liposomes [22]	16
Figure 2.2: Schematic representation of US energy deposition. HSP- heat shock potential; LTSLs- low temperature sensitive liposomes; SDT- sonodynamic therapy; ECM- extracellular matrix [54]	24
Figure 3.1: Schematic of the reaction for the synthesis of DSPE-PEG-pNP lipids	27
Figure 3.2: Preparation of calcein-containing DSPE-PEG-pNP liposomes from DPPC, cholesterol and DSPE-PEG-pNP.....	28
Figure 3.3: Reactions involved in the preparation of DSPE-PEG-Albumin liposomes	29
Figure 3.4: Apparatus used in the release experiments. (A) 20-kHz ultrasonic probe, (B) Fluorescence cuvette, (C) Fluorescence Spectrofluorometer.....	30
Figure 4.1: Average radii of DSPE-PEG-pNP control liposomes and albumin liposomes. The results were obtained by DLS measurements and the average \pm standard deviation of different technical replicates, are shown for 3 batches of each liposome type	33
Figure 4.2: A typical normalized online LFUS release curve from targeted liposomes.	34
Figure 4.3: Calcein release curves from DSPE-PEG-pNP control liposomes, triggered by 20-kHz pulsed US (20 s on 10 s off) at different power densities. Results are average \pm standard deviation of different liposome batches for each power density. The shaded areas are the error bars	35
Figure 4.4: Comparison of the initial release rates of calcein (A) and final release percentage (B) from control DSPE-PEG-pNP liposomes at different power densities.....	36
Figure 4.5: Calcein release curves from DSPE-PEG-albumin liposomes, triggered by 20-kHz pulsed US (20 s on 10 s off) at different power densities. Results are average \pm standard deviation of different liposome batches for each power density. The shaded areas are the error bars	38
Figure 4.6: Comparison of the initial release rates of calcein (A) and final release percentage (B) from DSPE-PEG-albumin liposomes at different power densities	39

Figure 4.7: Comparison of the release curves for control and albumin liposomes at (A) 6.08 W/cm², (B) 6.97 W/cm², and (C) 11.83 W/cm². Results are average ± standard deviation for 3 different liposome batches. The shaded areas are the error bars41

Figure 4.8: Comparison of the rates of calcein release from control and DSPE-PEG-albumin liposomes at different power densities. (A) after the second pulse of ultrasound; (B) final release42

List of Tables

Table 1.1: Cancer Statistics, United States, 2012. [4]	12
--	----

Chapter 1: Introduction

Cancer is a disease caused by an abnormal, uncontrolled cell growth, with the possibility of invasion of the neighboring tissues and organs [1]. Cancer starts in the body's basic unit of life, the cell. Figure 1.1 describes the division series of both normal and cancerous cells. Neoplasms and malignant tumors are other terms used to name cancer [2]. Cancer can be grouped into the following categories: carcinoma – cancers that start in the skin or tissues that cover organs; sarcoma –cancers occurring in connective or supportive tissues (e.g. bone and muscles); leukemia – cancer that originates in blood forming tissue; lymphoma and myeloma - cancers affecting the cells of the immune system; and central nervous system cancers [1].

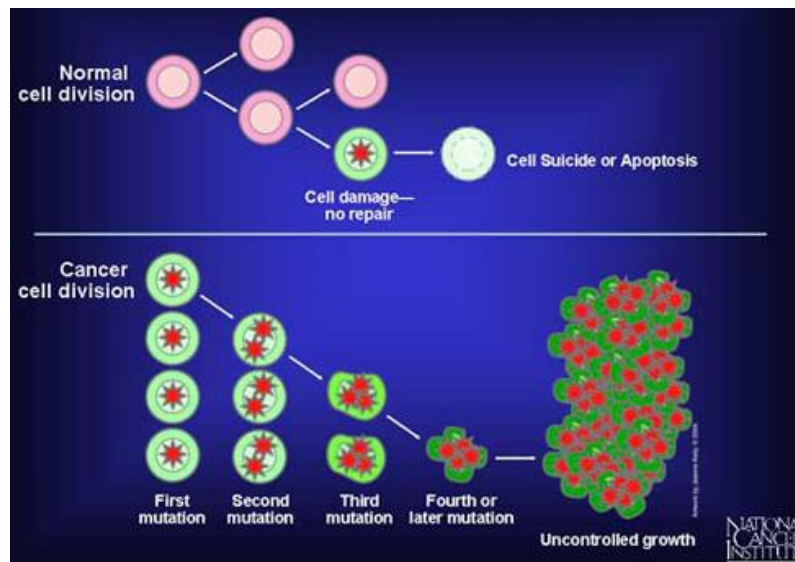


Figure 1.1. Schematic of cancer cell abnormal growth [1].

Cancer, which may be a lethal disease, is the second most common cause of death in the USA. Fifteen million cancer cases are predicted to be diagnosed by the year 2020, and around 12 million patients of cancer are expected to die [3]. Table 1.1 shows some significant 2012 cancer statistics in the United States. As can be seen, the three most commonly diagnosed cancers among men are prostate, lung, and colorectal cancers, whereas, breast, lung, and colorectal cancers are the most commonly diagnosed types among women. In addition, men have a higher probability of being diagnosed with cancer compared to women [4].

Table 1.1: Cancer Statistics, United States, 2012. [4]

Comparison	Women	Men
Most commonly diagnosed cancers	<ol style="list-style-type: none"> 1. Breast 2. Lung and Bronchus 3. Colorectal 	<ol style="list-style-type: none"> 1. Prostate 2. Lung and Bronchus 3. Colorectal
Lifetime probability to be expected with cancer	Lower	Higher
Overall cancer death rate decreased by	1.8%	1.6%

Cancer treatments fall under four categories: surgery, chemotherapy, radiation, antibody blocking therapy, or combinations of these [5]. Recently, researchers have been focusing on the study of more selective and effective cancer therapies which are a combination of chemotherapy, radiation and antibody blocking therapy, to reduce the impact of chemotherapeutic drugs on healthy cells.

Chemotherapy uses cytotoxic drugs to destroy the tumor, or to slow its growth [6]. Approved cytotoxic drugs are usually classified as: alkylators (the largest group), such as Melphalan; topoisomerase inhibitors, such as doxorubicin (Dox); antimetabolites such as Caldribine; microtubule interacting agents, such as Vinorelbine; and amino acid depletion agents, such as asparaginase [6]. These types differ in their mechanism of action to destroy or/and slow the growth of cancer cells. For example, asparaginase affects the cell membrane, since it hydrolyzes asparagine, an amino acid essential for cell and tumor growth. On the other hand, most cytotoxic chemicals, such as alkylators, interact with and preclude intercellular functions needed for cell survival. It is important to point out that frequent administration of cytotoxic drugs, such as Dox, may result in cardiac dysfunction [7].

Chemotherapy is administrated intravenously, orally, directly injected into the organ, or into the skin [8]. Chemotherapy can provide cure to some cancer patients, such as those suffering from acute leukemia. However, it does not necessarily assure a cure for other cancer types. Chemotherapy may improve the survival rate of some patients, particularly those suffering from breast or colorectal cancers. Furthermore, it may only provide tumor-associated symptoms of relief as it is the case with pancreatic cancer

patients. In other cases, such as in the case of thyroid cancer patients, tumors are poorly sensitive to chemotherapy [6].

Chemotherapy has many downsides, especially when administered by conventional methods, when it affects not only cancer cells, but also healthy (normal) cells [8, 9]. As a result, patients receiving chemotherapy often experience uncomfortable or even life threatening serious side-effects. Common side effects include hair loss, fatigue, nausea and vomiting [9]. Furthermore, chemotherapy mostly affects fast growing cells, hence, throat and mouth sores and skin problems are common among chemotherapy receivers [8]. In addition, chemotherapy affects the bone marrow which, as a result, hinders the production of red blood cells, white blood cells, and platelets. This usually leads to an increase of susceptibility to infections and an increase in the risk of bleeding [5, 6]. Besides, 70% of the patients treated with chemotherapy do not usually respond effectively to the initial administration of the anti-neoplastic agent. In turn, many patients build up a resistance after several administrations of the drug; a phenomenon caused by the cellular multi-drug resistance (MDR) [10].

Identifying many life threatening side effects of the conventional chemotherapy medication, such as its cardiotoxicity, and the MDR effect, has motivated researchers to look for new pharmacological medication approaches. A recent trend in cancer treatment is the use of drug delivery systems (DDS) using nanoparticles as drug carriers. Nanoparticles are a distinct collection of molecules with a size range of 1 nm to 1 μ m [11, 12]. Nanocarriers encapsulate a variety of therapeutic agents, including small hydrophilic/hydrophobic molecules, peptides, and nucleic acids. The encapsulated molecules can then be released from the carrier in a controlled manner over a given period of time. Furthermore, due to the small size of the nanocarriers, transport across biological barriers can be enhanced, hence facilitating cellular uptake. In addition, the surface of the nanocarrier can be modified to increase the blood circulation half-life [12]. Another advantage of using nanoparticles is that they are biodegradable [13]. Nanocarriers may be designed to be highly specific, allowing the controlled targeting of cancer cells, thus decreasing the cytotoxicity of the therapeutic agent on healthy cells [7]. They also contribute for a reduction in chemotherapy cost and side effects on the patient's organs. Another advantage of using nanocarriers is that they have a higher

therapeutic index for the agent at the tumor [12], which can improve imaging and detection of tumors when carrying imaging agents besides the drug [14].

Using carefully designed nanoparticles, it is possible to control the time and space in which the drugs are released [15, 16]. This is attained using nanoparticles that are *targeted* to a certain type of cancer cells. After their accumulation at the tumor site, the release of the drugs they encapsulate is *triggered* by the application of a stimulus to which the nanoparticles respond.

The nanoparticles developed in this work are liposomes, vesicles composed of lipid bilayer(s) which surround(s) an aqueous core. Liposome sizes range between 0.05 and 1 μm [17]. Hydrophilic drugs can be encapsulated in the inner aqueous interior, whereas hydrophobic drugs can be carried within the lipid bilayer [18] (Figure 1.2 (a) and (b)). The liposomes were designed to target cancer cells overexpressing receptors for albumin on their surface, hence a human serum albumin (HAS) moiety was conjugated to the liposome structure.

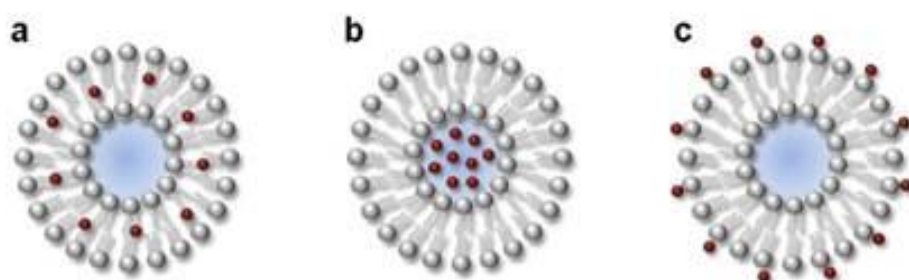


Figure 1.2. Schematic representing the structure of liposomes. (a) encapsulating hydrophobic drug; (b) encapsulating hydrophilic drug; (c) modified with ligand or moiety [18].

The release of the encapsulated molecules from the liposomes was triggered using ultrasound (US). The applications of US waves in medicine are well known and include diagnostic imaging, kidney stone disruption, blood flow analysis, drug delivery, and tumor ablation [19]. An application of US emerging in biotechnology is the use of ultrasound contrast agents (UCAs) in diagnostic US imaging. They are called UCAs due to their acoustic impedance being different from that of the soft tissue [20]. Ultrasound frequencies used for such applications usually range between 0.8 and 3 MHz [21]. In actuated drug delivery, US is used as a triggering technique to enhance drug release to

specific cancer cells. It is attractive for use in DDS due to two phenomena: hyperthermia (temperature effects) and cavitation (mechanical effects).

Liposomes and other nanoparticles, as well as US, will be discussed in more detail in the following chapter.

Chapter 2: Literature Review

2.1. Nanoparticles as Drug Delivery Systems

Using nanoparticles to encapsulate chemotherapeutic agents and to deliver these therapeutic agents to the tumor site is a promising treatment for cancer. Nanoparticles used as carriers in DDS for cancer therapy include micelles, nanoemulsions, dendrimers, and liposomes, among others [11]. This work will focus on liposomes as drug nanocarriers, but other nanoparticles are also briefly discussed in this chapter.

2.1.1. Liposomes.

In general, lipids used to prepare liposomes are found naturally in the human body, and include DSPE (1,2-distearoyl-*sn*-glycero-3-phosphoethanolamine), HSPC (hydrogenated phosphatidylcholine from soybean lecithin), phosphatidylglycerol, and DSPC (1,2-distearoyl-*sn*-glycero-3-phosphocholine) [12]. Liposomes are classified according to their lipid bilayer structures as unilamellar vesicles (ULVs) and multilamellar vesicles (MLVs). The former can be further classified according to their size as small unilamellar vesicles (SUVs), giant unilamellar vesicles (GUVs), and large unilamellar vesicles (LUVs), as represented in Figure 2.1.

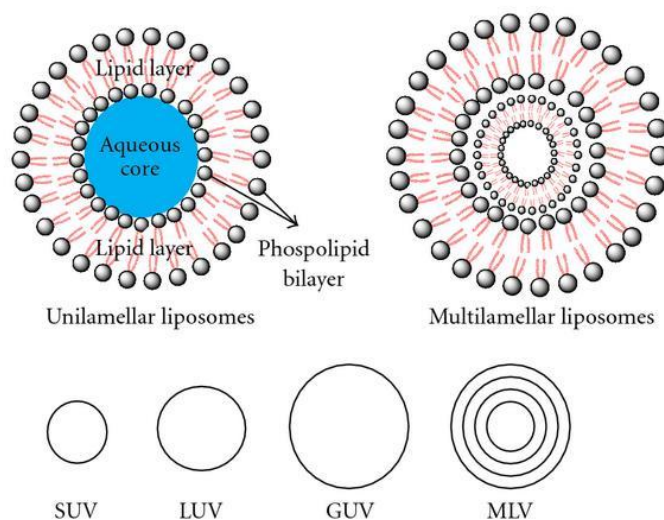


Figure 2.1. Schematic depicting structures and types of liposomes [22].

Liposomes can be modified by varying the liposome lipid composition. For example, it was observed that liposome formulations containing hydrogenated phosphatidylinositol (HPI) and monosialoganglioside (GM) had the highest tumor cell

drug uptake among other examined liposome compositions [23]. Another modification can be done by adding anionic phospholipid [24], and by changing the amount of cholesterol in the liposome [25] (Figure 1.2 (c)).

Liposomes have many advantages that make them attractive nanocarriers [18]: (i) they are structurally stable; (ii) they are stable in biological fluids (e.g. blood); (iii) they have a long shelf life; and (iv) their size can be customized. Moreover, liposomes may be coated with polyethylene glycol (PEG) or other polymers, which increase their circulation time. These carriers are called *stealth* liposomes [26]. Polyethylene glycol is a safe and non-toxic compound that has been approved by the FDA. It may form a mushroom-like structure or a brush-like structure on the surface of the liposome, depending on its molecular weight and surface density [13]. These coatings prevent the opsonization of the liposomes by inhibiting their recognition by phagocytes. As a result, they prolong the circulation half-life of the nanovehicles in the body, and decrease their degradation by metabolic enzymes [18, 27, 28].

Liposomes can be further modified to selectively increase the drug accumulation in the desired location. These *targeted* liposomes are prepared by conjugating moieties to the surface of the liposome, allowing them to recognize and bind to specific receptors on the surface of cancer cells. Examples of molecules that can be used as ligands or targeting moieties are: antibodies and their fragments, lectins, albumin and other proteins, lipoproteins, hormones, charged molecules, monosaccharides, oligosaccharides, polysaccharides, and some low-molecular-weight ligands, with folic acid being the most common [26]. The main advantages of using targeted liposomes over plain liposomes include a dramatic increase in the amount of drug delivered to the target site and the so-called “bystander killing” effect, caused by the diffusion of the drug molecules to adjoining tumor cells [29].

It is important to point out that liposomes have three main limitations. First, liposomes are mainly used to encapsulate hydrophilic drugs, since the incorporation of hydrophobic drugs in their lipid bilayer may disturb their stability. Second, the drug needs to leak from a liposome that has been designed to be stable [18]. Third, the carried drug cannot be re-encapsulated after release, unlike in micelles (see 1.3.2) [17].

2.1.2. Micelles.

Micelles are spherical nanoparticles with a diameter ranging from 5 to 100 nm, resulting from the self-assembly of amphiphilic molecules in an aqueous solution, originating a structure with a hydrophilic or polar corona and a hydrophobic core [30]. Hydrophobic drugs can penetrate and accumulate inside the hydrophobic center which decreases the interaction with the aqueous exterior [11, 17]. Advantages of micelles include their easy preparation methods (usually just dissolving the copolymers in an aqueous solution), simple drug loading (just by mixing the micelles with the drug), and their stability and controllability [30]. However, it was observed that when injected intravenously, some micellar formulations suffered a rapid clearance by the mononuclear phagocyte system. Thus, such micelles must be modified by coating them with agents, such as the previously mentioned PEG [30].

The most structurally stable micelles are polymeric micelles, which are used in most DDS. These micelles are diblock, triblock or even more complex structures of copolymers [17]. Pluronic® micelles, composed of poly(ethylene) oxide and poly(propylene) oxide blocks, have been widely studied as nanocarriers [11]. They are particularly important in acoustically activated drug delivery because one of their members, Pluronic® P105, has been extensively studied to deliver Dox in conjugation with ultrasound [17]. They are formed even at very low polymeric concentration, hence they are very stable due to their slow dissociation, which ranges from hours to days [17]. Additionally, their size allows them to extravasate at the tumor site, due to the enhanced permeability and retention (EPR) effect, while escaping renal excretion [31].

2.1.3. Dendrimers.

Dendrimers are three-dimensional, synthetic, highly branched, polymeric macromolecules. They are spherical in shape with layers of branches around the core. Dendrimers have some attractive properties to drug delivery applications: they are water soluble, have uniform size, include inner cavities and their surfaces, and can be modified according to their functions [32]. In addition, their biocompatibility, polyvalence and precise molecular weight make them ideal nanocarriers for drug delivery applications [33]. Dendrimers can carry both hydrophilic and hydrophobic drugs. Common types of dendrimers are poly(propylene imine) (PPI), polylysinedendrimers and the first synthesized and commercialized dendimer, poly(amidoamine) (PAMAM) [32]. A study

by Kitchens *et al.* reported that PAMAM was transported through the bio-membranes by paracellular and endocytosis processes [33].

2.1.4. Nanoemulsions.

Emulsions can be defined as a mixture of two insoluble liquids, one of which is the continuous phase while the other liquid is the dispersed phase [11]. The simplest example of an emulsion is oil-in-water. The droplet diameter ranges from 50 to 1000 nm [34]. In drug delivery, the continuous phase is usually aqueous and the dispersed phase is where the hydrophobic drug is carried [11].

Nanoemulsion research attracts many researchers because nanoemulsions have small droplet sizes which allows easier extravasation when releasing drug [35] and causes large reduction in gravity, and no sedimentation occurs on storage [34]. In some applications, it can be used as a substitute for liposomes.

2.1.5. Protein-bound paclitaxel.

Protein-bound paclitaxel is a nanoparticle that carries paclitaxel into cancer cell. It is used to treat breast, lung, prostate and other cancers [36, 37]. Although conventional paclitaxel has also been used in the treatment of cancer, it has some drawbacks, such as the fact that it relies on solvent-based delivery carriers injected intravenously, which can cause serious toxicity. Thus, a nanocarrier protein-engineered therapy is advantageous. Using protein-bound paclitaxel nanocarriers, one can avoid the need for premedication and prolonged administration time. It can also increase the ease of administration. The first approved protein bound paclitaxel by FDA is albumin-bound paclitaxel called NabTM-paclitaxel, which is administrated over a short period of time and does not need intravenous tubing [36].

2.2. Targeted Drug Delivery Systems

An active pharmaceutical ingredient (API), when administrated to a patient, is distributed within the body proportionally to the blood flow. Furthermore, along its journey to the site of action, the API has to cross many organs, tissues and cells, where it can be deactivated. Otherwise, it can lead to undesirable effects for sites that are not meant to be reached. Thus, to ensure that the drug reaches the target site, it has to be administrated in large amounts. This will cause many negative effects on healthy cells, especially if the drug is cytotoxic and in the best case it is wasted in normal tissues

causing an increase in therapy cost, according to Torchilin [26]. A solution to such problems can be introduced using drug targeting. Drug targeting can be defined as an increase in the selective and quantitative accumulation of an API in a certain tissue or organ in the body, thereby reducing side effects of unspecific drug accumulation. The interaction of four main components makes the targeted delivery possible: chemotherapeutic ingredient, targeting moiety, carrier (i.e. nanoparticle), and a target. In this work, calcein (a mimic drug) simulates the use of the chemotherapeutic ingredient, while human serum albumin (HSA) is used as the targeting moiety, and liposomes as carriers

Nanoparticles can also be designed to release drug by external stimuli such as magnetic fields or US, which is a process called *triggered* targeting. Others are sensitive to changes in pH or temperature which can be used to administer a drug into a target area with a different pH and temperature. The research presented here reports on the use of 20-kHz low frequency US (LFUS) as a trigger to release calcein encapsulated in the prepared liposomes.

2.2.1. Passive targeting.

The vasculature of tumor cells differs from that of healthy cells in their functionality and morphology. In tumors, the blood vessels have defective vaso-architecture, including irregular shapes, and lack of smooth muscle layer. The endothelial cells are also not well organized. Furthermore, they are dilated, wide and leaky. The basement membrane in the tumor is usually abnormal or even absent in some cases. Additionally, tumors have impaired lymphatic drainage of macromolecules and lipids [38, 31, 39].

These characteristics of tumor tissues led to an enhanced permeability and retention (EPR) effect that allows extravasation of drug-loaded nanoparticles in tumor cells [30]. The EPR effect can be observed with molecules that have long plasma half-lives, with an apparent size higher than 50 kDa, above the kidney clearance threshold (5 nm) [31, 40]. Moreover, the molecule should be neutral or anionic but not cationic, because the inner surface of blood vessels is highly negatively charged [31]. The EPR effect is usually characterized by imaging tumor blood volume and flow [40]. When the delivery essentially only relies on the pathophysiological properties of the target cancer tissue, as in non-ligand nanoparticles, it is referred to as the *passive* drug targeting.

One of the most meaningful examples of passive targeting carriers approved for clinical use is Doxil®. It is an echogenic PEGylated liposome loaded with Dox and used in the treatment of many cancer types, including ovarian cancer, breast cancer, and hormone-refractory prostate cancer (HRPC) [41]. Other examples include Myocet (non-PEGylated liposome-Dox) and Daunoxome (non-PEGylated liposomal daunorubicin) [42]. Even with PEGylated liposomes, less than 5% of the administered drug accumulates in tumor cells by passive targeting [30].

While most of the drugs have a plasma half-life of 20 minutes in humans and mice, it takes around 6 hours of circulation for any drug to exert the EPR effect [31]. Thus, researchers studied the improvement of the EPR effect by using the *stealth* liposomes mentioned previously, and other modified liposomes.

2.2.2. Active targeting.

Active targeting is a type of targeting achieved by conjugating the carrier with another molecule (called *ligand* or *targeting moiety*) to actively deliver the drug to tumor cells. It is particularly important when passive targeting is not possible or sufficient. This occurs when vascular permeability, pH, and temperature of the affected area do not significantly differ from that of normal tissues [26]. Also, active targeting is employed in targeting within the circulatory system [30]. One of the most important advantages of active targeting is the effective delivery of high loads of drugs avoiding MDR [5].

The simplest approach to prepare targeted drugs includes direct coupling of a drug to a targeting moiety. The most common examples of such approach are immunotoxins, where a natural toxin is split into active and recognizing moieties. The active moiety is the toxic part that is conjugated with an antibody. Another approach which is of interest in this research includes the use of a nanocarrier, e.g. liposomes. The liposome can be modified by conjugation with a targeting moiety. The targeting moiety or ligand should be able to recognize certain binding sites on the tumor cell surface, so that the carrier remains attached to the surface, and releases its drug load upon request [43].

The scope of this research was to synthesize PEGylated liposomes with their surface modified by covalently bound albumin. Human serum albumin (HSA) is a naturally occurring protein in human plasma, and it is produced in the liver [44]. Human serum albumin was previously studied as a drug carrier molecule by itself, such as

albumin-bound paclitaxel. Albumin is a natural carrier of hydrophobic molecules. Another example of albumin as a nanocarrier was described by Dreis and co-workers [45]. They studied the loading of Dox to HSA nanoparticles by two methods: adsorption and incorporation into the particle matrix. Both strategies resulted in nanoparticles with a size range of 150 nm and 500 nm. The loading efficiency was reported to be as high as 95%. Additionally, Vuarchey *et al.* [46], reported the preparation of PEGylated-liposomes targeted with albumin (PEG-L-A), but using a different method from the one used here.

2.2.3. Ultrasound-triggered release from liposomes.

After a targeted liposome reaches the cancer site, a stimulus is needed to trigger the release of the encapsulated drug. This is called *actuated* targeting, which involves the use of external triggers, such as electric or magnetic fields, pH or temperature changes, as described previously. Ultrasound has been widely researched as a trigger mechanism for US-sensitive liposomes, called echogenic or acoustically active liposomes (AAL).

Ultrasound is composed of pressure waves with frequencies higher than 20 kHz. It is generated by a piezoelectric transducer that changes applied voltage into mechanical movement. Ultrasound waves can be focused, refracted, and reflected, and they can be absorbed differently by various media [47]. Clinically, US is used in imaging, physical therapy [48], and hyperthermic cancer therapy [49, 50]. Ultrasound frequencies used for such applications usually range between 0.8 and 10 MHz [21].

Ultrasound has many advantages over other release techniques. It is widely employed in the medical field due to its low cost, safety and simplicity. An exposure to high-intensity high-frequency US for 2 minutes results in a temperature elevation of 4 to 5 °C, which is below the cytotoxicity level [51]. As stated by Pitt *et al.* [30] ultrasound has the ability to propagate into deep tissue, while optical waves cannot; US can be controlled in time and space, focused directly on the tumor cells without affecting healthy tissues. Furthermore, it is noninvasive, hence no surgery or insertion is needed. In addition, it has been reported that US enhances drug delivery to solid tumors up to 10-fold, when compared with delivery in its absence [52]. Most importantly, it was described that US-actuated targeting has the ability to produce effects on tumor tissues

that synergize with other delivery methods – passive and active. The synergistic effect occurs due to cavitation effects [53].

The energy of US, when focused on a specific area, will usually dissipate in heat generation, acoustic cavitation, and radiation forces [54] (Figure 2.2). In targeted drug delivery, US can be employed due to two phenomena: hyperthermia and cavitation. Hyperthermia occurs when the US beam is focused on a small tumor tissue area, and hence the power/area (called *intensity* or *power density*) becomes very high resulting in its heating. When using liposomes as a DDS, when the temperature increases beyond the phase transition temperature of the lipid, the lipid bilayer opens and the encapsulated drug is released [55]. It was also reported that the thermal energy from heating may be employed in releasing the drug encapsulated in liposomes and in ablating the tumor [47]. However, US with low frequency and intensity, which does not cause cavitation, has little or no effect on the enhancement of cellular drug delivery [47]. Cavitation can be defined as the formation and/or activity of gas bubbles in a medium exposed to US [56]. The gas bubbles will expand at low pressure and will contract at high pressure. There are two types of cavitation depending on the bubble size stability: *stable* and *inertial* cavitation. Stable cavitation creates a circulating fluid around the bubble with velocities and shear rates proportional to the oscillation amplitude. If the shear stress exceeds that of the liposome, it will rupture and release the drug from this nanocarrier [47]. On the other hand, at very high intensity and microbubble concentration, inertial cavitation occurs [55]. In this case, the gas bubbles collapse causing a liquid jet release at sonic speed, which can pierce the cell endothelial layer. This can explain the increase in membrane permeability upon US application [57].

Using US as a trigger, it is possible to control several factors that influence the release of the drug, such as the power input, ultrasonic intensity, the duration of sonication, and the position of the US source [58].

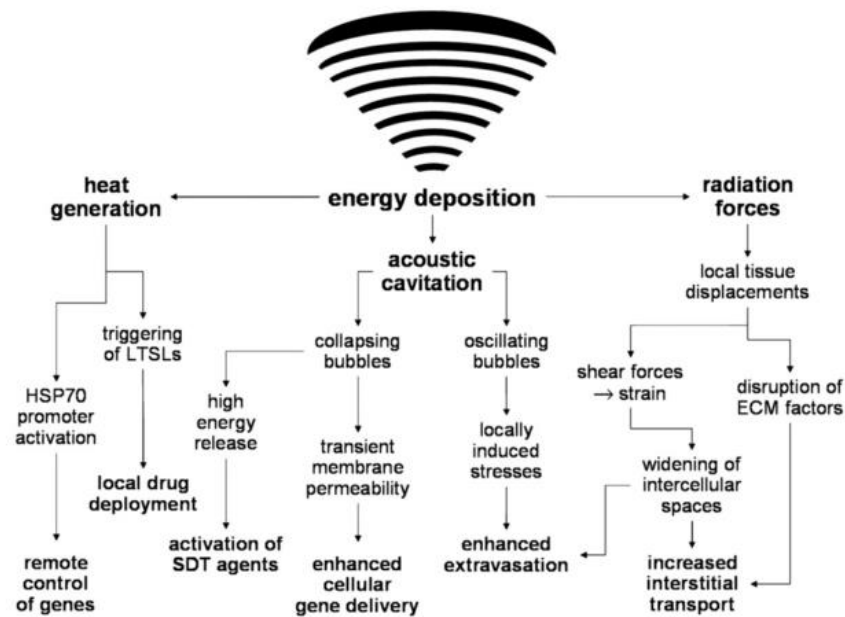


Figure 2.2: Schematic representation of US energy deposition. HSP- heat shock potential; LTSLs- low temperature sensitive liposomes; SDT- sonodynamic therapy; ECM- extracellular matrix [54].

2.3. Relevant *in vitro* Studies

Many researchers have conducted several *in vitro* experiments to test the effectiveness of drug delivery from various types of liposomes. In this section, *in vitro* studies related to this thesis will be reviewed to examine the effect of targeted liposomes, albumin-targeted liposomes, and of US on drug release and uptake.

Low and Lee [27] examined the delivery of the anticancer drug Dox from folate-targeted liposomes, by measuring the change in Dox fluorescence using a spectrofluorometer. The results showed that the uptake of folate-PEG-liposomes by KB human oral carcinoma cells was 45 times higher than that of non-targeted liposomes.

Another research, by Vuarchey *et al.* [46], reported a new approach to macrophage-specific drug delivery by PEGylated-liposomes targeted with albumin (PEG-L-A). Macrophages contribute to tumor growth, and hence effective targeting of drugs to such cells may provide a good approach for the treatment of some types of cancer. The study analyzed the drug uptake by macrophage cells using fluorescence microscopy and flow cytometry. It was found that the macrophage uptake of PEG-L-A was about 17-fold higher after 1 hour incubation and remained 4 times higher after 24 hours, when compared to that of plain liposomes. Moreover, compared to PEGylated-

liposomes, PEG-L-A cell uptake was 53 folds higher after 1 hour and 9 times higher after 24 hours. In addition, the research examined the effect of different types of albumin coated liposomes, such as murine (MSA), bovine (BSA) and human serum albumin (HSA). No significant differences could be observed when comparing the uptake of liposomes targeted with the three different types of albumin. Hence, it was concluded that the uptake was independent of the antigenicity of a foreign protein.

Huang and McDonald [59] compared the release from AAL, containing both air bubbles and calcein, with other types of liposomes, including air-only liposomes and calcein-only liposomes. In addition, they examined if high frequency US (HFUS) could trigger the release from AAL. They used 1-MHz HFUS, and a variety of intensities and duty cycles, and observed that the highest release conditions were obtained at 2 W/cm², and 100% duty cycle for 10 s. Under these conditions, AAL released a much higher amount of drug than non-AAL.

2.4. Relevant *in vivo* Studies

In vivo research usually employs rats and mice models (and other larger mammals). There are several *in vivo* drug delivery studies which examined the effect of encapsulating Dox in liposomes, a drug commercialized under the name Doxil®. The results showed that Doxil® has a higher half-life than Dox encapsulated in non-PEGylated liposomes, and also higher than that of free Dox [41, 60].

Recent studies reported the effect of coating liposomes with different ligands such as proteins. Common tested proteins are immunoglobulin G and fibronectin, well known opsonins that enhance the hepatic disposition of liposomes [61]. On the other hand, other studies [62, 63] tried to identify proteins with dysopsonic activity in drug delivery. Rat serum albumin (RSA) was the selected protein to be coupled onto the surface of PEGylated liposomes (PEG-L-RSA). The research aimed to study and compare the hepatic disposition of non-PEGylated liposomes, PEGylated liposomes and PEG-L-RSA in rats. It was revealed that the plasma concentration of PEG-L-RSA was the highest, 3 times greater than that of non-PEGylated liposomes. Hence, it was concluded that RSA decreased the hepatic clearance of liposomes. However, for spleen, both PEGylated liposomes and PEG-L-RSA showed the same clearance level [62]. In addition, it was found that Dox accumulation in the heart was less for PEG-L-HSA than for free Dox [63].

Another important study reported the drug delivery to mice tumors triggered by US [64]. In the study, a first group of mice, which received a liposome-encapsulated Dox (Doxil®) injection into their tails veins, were exposed to high intensity US. A second group was injected with Doxil®, but was not exposed to US. A third control group received no treatment. After removing tumors and assaying the Dox accumulation content, it was observed that the Dox concentration in the tumors of the first group was 124% higher than that of the second group. Hence, from this study, it was concluded that the delivery of liposomal Dox to tumors treated with high intensity US is an effective method of drug delivery.

Chapter 3: Experimental Procedures

3.1. Chemicals and Reagents

Dipalmitoylphosphatidyl choline (DPPC) and 1,2-distearoyl-*sn*-glycero-3-phosphoethanolamine-N-[amino(polyethylene glycol)-2000] (ammonium salt) (DSPE-PEG(200)-NH₂) were obtained from Avanti Polar Lipids Inc. (Alabaster, AL, USA). 4-Nitrophenyl chloroformate (pNP), human serum albumin (HSA), calcein disodium salt, and the bicinchoninic acid (BCA) kit were obtained from Sigma-Aldrich Chemie GmbH (Munich, Germany). Triethylamine (TEA) was obtained from Riedel-de Haen, while cholesterol was from AlfaAesar (Ward Hill, MA, USA). All other reagents were of analytical grade.

3.2. Methodology

3.2.1. Preparation of DSPE-PEG-pNP control liposomes.

These liposomes were prepared using DSPE-PEG-pNP, cholesterol and DPPC. The first step was the synthesis of DSPE-PEG-pNP, prepared by the reaction of pNP with DSPE-PEG-NH₂ as shown in Figure 3.1. The reaction was incubated overnight at room temperature with stirring.

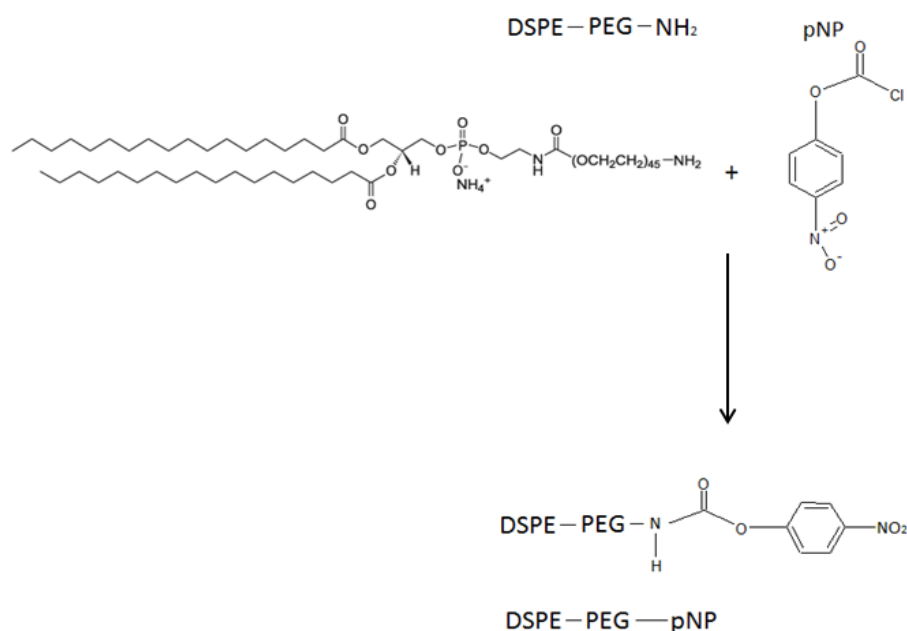


Figure 3.1: Schematic of the reaction for the synthesis of DSPE-PEG-pNP lipids.

The liposomes were prepared by a modified version of Torchilin protocol [65], using DSPE-PEG-pNP, cholesterol, and DPPC in a molar ratio of 5:30:64. The reagents were dissolved in 4ml of chloroform, which was subsequently evaporated under vacuum in a rotary evaporator (Heidolph, Laborota 4003), until a thin film formed on the walls of the flask. Afterwards, the film was hydrated with 2 mL of 30 mM calcein solution, with the pH adjusted to 5.2. The solution was then sonicated at 40-kHz in a sonicator bath (Elma D-78224, Melrose Park, IL, USA) for 15 minutes, and then extruded three times (10x each, changing the filters in between) using the Avanti® Mini-extruder with 0.2 μm polycarbonate filters (Avanti Polar Lipids, Inc., Alabaster, AL, USA). All steps from evaporation to extrusion were performed at 55°C to make sure that it is above the DSPE transition temperature T_m . The transition temperature can be defined as the temperature where structural changes in the lipid membrane occur as it transfers from a gel to the liquid-crystalline phase [66]. Finally, the solution was cleaned from calcein and salts by size-exclusion chromatography in a Sephadex G-100 column (GE Healthcare Life Sciences, Pittsburgh, PA, USA) previously equilibrated with PBS pH 7.4. The turbid liposome fractions were collected. Figure 3.2 shows a schematic for the described liposome preparation. The liposome solution was kept at 4°C in PBS buffer until use.

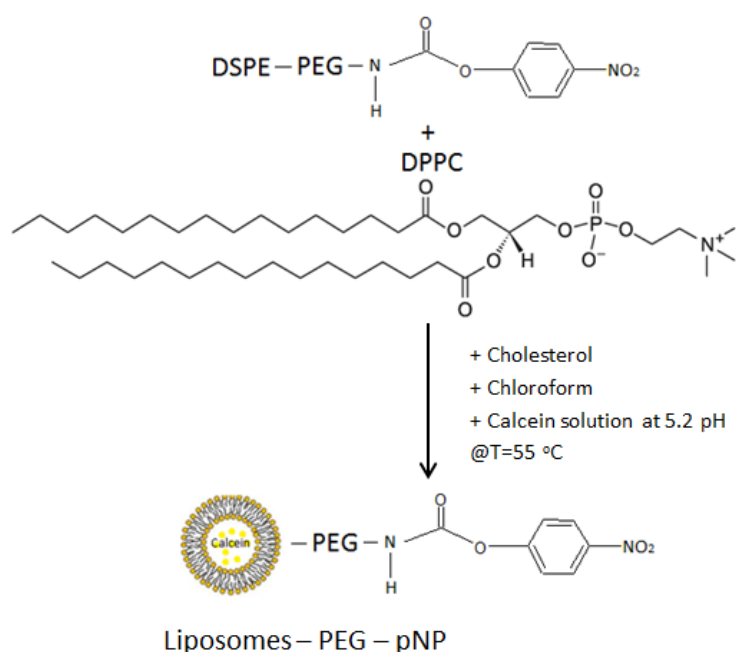


Figure 3.2: Preparation of calcein-containing DSPE-PEG-pNP liposomes from DPPC, cholesterol and DSPE-PEG-pNP.

3.2.2. Preparation of DSPE-PEG-Albumin targeted liposomes.

The targeted liposomes were prepared by the reaction of the DSPE-PEG-pNP control liposomes with albumin, as shown in Figure 3.3. First, 0.5 ml of a HSA solution (2 mg/ml in sodium borate buffer pH 8.5) were added dropwise to 1.5 ml of the DSPE-PEG-pNP liposome solution in PBS pH 7.4, prepared as described in 3.2.1. The pH was adjusted to 8.5 by the addition of a controlled volume of 1 M NaOH. The reaction mixture was kept in a round-bottom flask covered with aluminum foil, and was stirred at room temperature overnight. The liposome solution was then cleaned by size-exclusion chromatography in a Sephadex G-100 column pre-equilibrated with PBS pH 7.4. The turbid fractions containing the liposomes were collected, and kept at 4°C in PBS buffer until use.

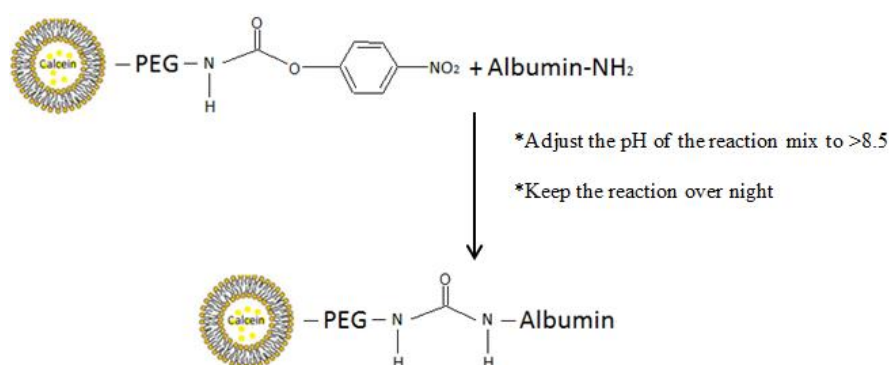


Figure 3.3: Reactions involved in the preparation of DSPE-PEG-Albumin liposomes.

The presence of albumin in the liposome sample was tested using the BCA assay kit, according to the instructions of the manufacturer [67]. A sample of DSPE-PEG-pNP control liposomes was used as a negative control.

3.2.3. Determination of the liposome size by dynamic light scattering.

The size distribution of liposomes is commonly determined by dynamic light scattering (DLS), electron microscopy, right angle light scattering and turbidity.

In this work, DLS, using the DynaPro® NanoStar™ model from Wyatt Technology Corp. (Santa Barbara, CA, USA), was used to determine the size of the prepared liposomes. The samples for measurements were diluted in PBS (pH 7.4). Dynamic light scattering autocorrelation data were analyzed using the software Dynamics7 – Static, Dynamic, and Phase Analysis Light Scattering, with both cumulant and regularization fits [68].

3.2.4. Release experiments.

Release experiments were done online, by continuously measuring the fluorescence using the QuantaMaster QM30 Phosphorescence/Fluorescence Spectrofluorometer (Photon Technology International, Edison NJ, USA). Due to the high cost of Dox, and for safety reasons, the model drug calcein was used to prepare the liposomes, and to follow the US-induced release. The spectrofluorometer measures the changes in calcein fluorescence over time, at an excitation wavelength of 494 nm and emission at 515 nm (determined as the best for liposome-encapsulated calcein) [69]. The sample dilution was made directly in a fluorescence cuvette, which was then placed in the sample chamber inside the spectrofluorometer. The 20-kHz ultrasonic probe (model VC130PB, Sonics & Materials Inc., Newtown, CT, USA) was introduced through the opening in the top-cover of the fluorometer and immersed inside the sample, 2 mm into the liquid in the cuvette (Figure 3.4). The initial fluorescence baseline (F_0) - before sonication and release of the drug started - was recorded for 60 s. The US treatment was then started and the fluorescence increase over time (F) was monitored until it reached a constant value. At this point, the sonication was stopped and the detergent Triton X-100 was added to fully lyse the liposomes, thus releasing the total amount of encapsulated calcein (F_{Tx}). The percentage of calcein release at each time point could then be calculated using the following equation:

$$\%Release = \frac{F - F_0}{F_{Tx} - F_0} * 100\%$$

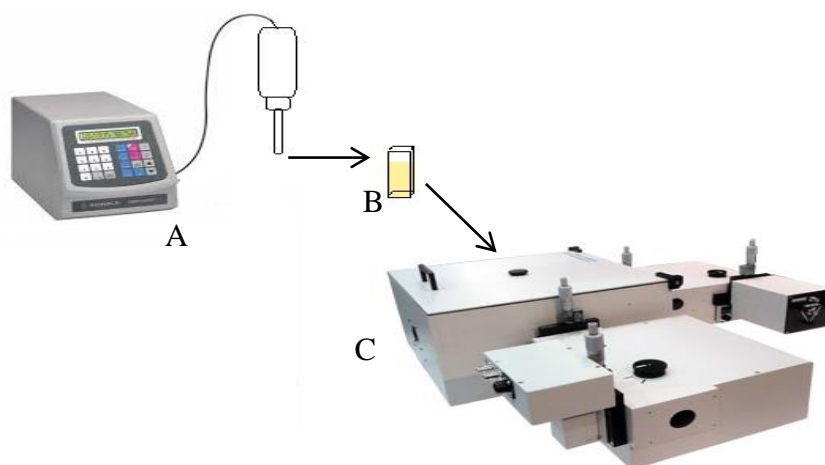


Figure 3.4: Apparatus used in the release experiments. (A) 20-kHz ultrasonic probe, (B) Fluorescence cuvette, (C) Fluorescence Spectrofluorometer.

Different concentration solutions of Tx100 and liposomes were prepared previously by our research group [69] to study the detergent-to-lipid ratio needed to reach a complete lysis of liposomes. It was concluded that the total release was obtained by adding Tx100 to a final concentration of 0.48 mM to an insonated sample. Furthermore, the buffer solution selection is critical and was studied previously. It was reported that a pH 7.4 buffer must be used to avoid calcein self-quenching and aggregation that occur at acidic pH, and also because this is the pH at which the *in vitro* cellular assays will be performed. Hence, all release experiments were performed at pH 7.4, using a final Tx100 concentration of 0.48 mM to lyse the liposomes. The data, which was normalized using the previous equation, were used to study the release curves. Initial rates of release were calculated as the percentage of release after the second sonication pulse (40 s of total sonication). The final percentage of release was calculated as the maximum normalized value of the stable part of the release curves. Several factors may affect the US-induced release from liposomes, including US pulse duration, power density, and liposomes related factors, such as their concentration in the sample, gas encapsulated, and composition [70]. Therefore, the experiments were repeated by varying the power density and frequency to determine the optimum release conditions.

3.2.5. Statistical analysis.

Means and standard deviations were calculated in Excel 2010. Pairwise comparisons were performed using two-tailed t-tests with the assumption of equal variances of the two samples. Two values were considered significantly different when $p < 0.05$ (unless otherwise stated).

Chapter 4: Results and Discussion

4.1. Liposome Size

The presence of albumin in the targeted liposomes was tested using the BCA assay, as referred previously. The DSPE-PEG-pNP liposomes were used as a negative control to discount any interference that the assay may have with other liposomal components. After ensuring that the protein was attached, the size of 3 batches of DSPE-PEG-pNP control liposomes and 3 batches of albumin targeted liposomes were determined by DLS, as described in 3.2.3.

The average radii for each liposome batch were calculated and are shown in Figure 4.1. The average diameter for control liposomes was determined as 208.52 ± 11.50 nm (calculated from the 3 liposome batches shown in blue in Figure 4.1). The albumin liposomes are larger particles with a diameter of 218.27 ± 12.73 nm (calculated from the 3 liposome batches shown in red in Figure 4.1). This confirmed that the synthesized liposomes of both types are LUVs. Although the albumin liposomes have a higher diameter than the control nanocarriers, a statistical comparison of the results showed no significant differences ($p = 0.38$), which is in accordance with a previous study reporting that for liposomes with a diameter greater than 200 nm, the albumin coupling did not significantly increase the size of the liposomes [62].

Vuarchey *et al.* [46] reported a lower diameter size for both types of liposomes. PEGylated liposomes were reported to have an average diameter of 111.3 ± 59 nm, while bovine serum albumin-liposomes were reported to have an average diameter of 151.1 ± 1 nm. These liposomes had a different composition and were prepared using a different method, hence it is expected that the results are different from the ones reported in this work.

In addition, since the particle diameter is around 200 nm, such liposomes, if used in *in vivo* experiments, are expected to be efficient for drug delivery because they have the ideal size to experience the EPR effect.

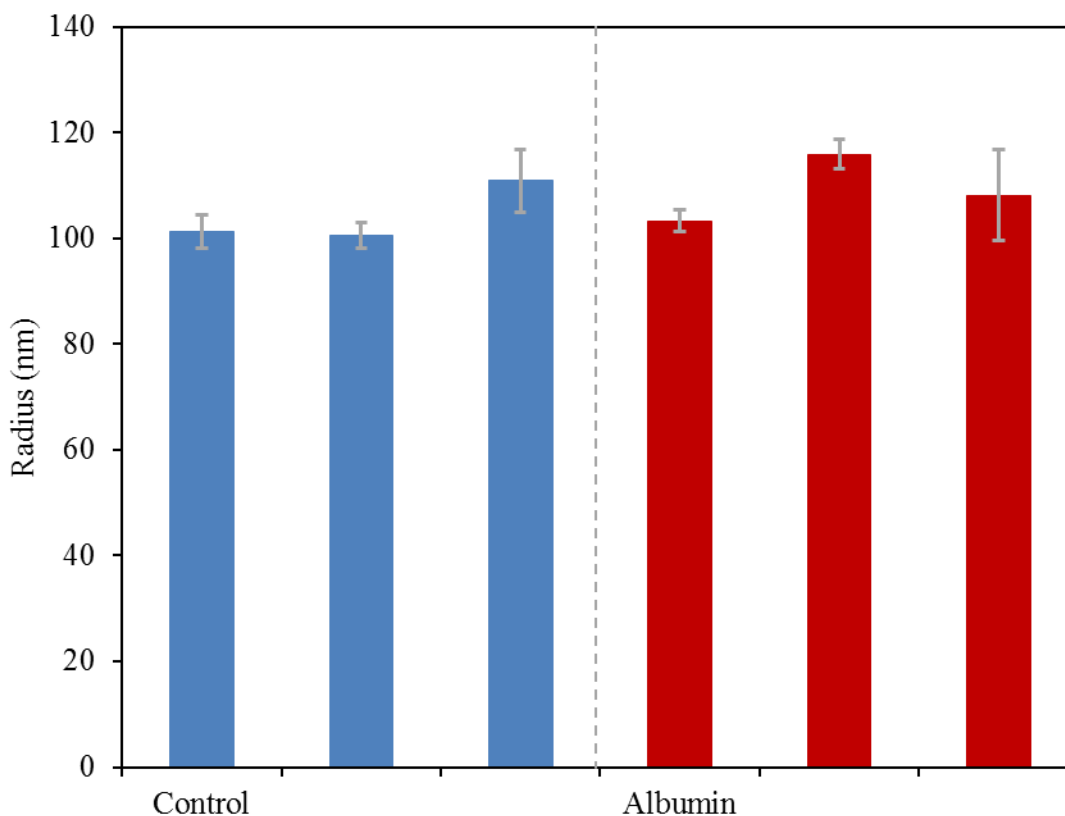


Figure 4.1: Average radii of DSPE-PEG-pNP control liposomes and albumin liposomes. The results were obtained by DLS measurements and the average \pm standard deviation of different technical replicates, are shown for 3 batches of each liposome type.

4.2. Online Low Frequency US (LFUS)-induced Release

All LFUS release experiments were performed at a fixed input frequency of 20 kHz and in PBS buffer pH 7.4. Release curves were obtained for 3 batches of every liposome type, at 3 different power densities: 6.08, 6.97 and 11.83W/cm². A typical release curve is shown in Figure 4.2. Before the application of US, the curve started with a baseline which measures the fluorescence level in the sample. When the sonication started, the fluorescence level increased due to the calcein release. Ultrasound was applied for 20 s, followed by a 10 s *off* period where a constant fluorescence level was measured, since there was no calcein release. The 20s *on* - 10s *off* cycle was repeated until a plateau was reached, and no more calcein release could be observed.

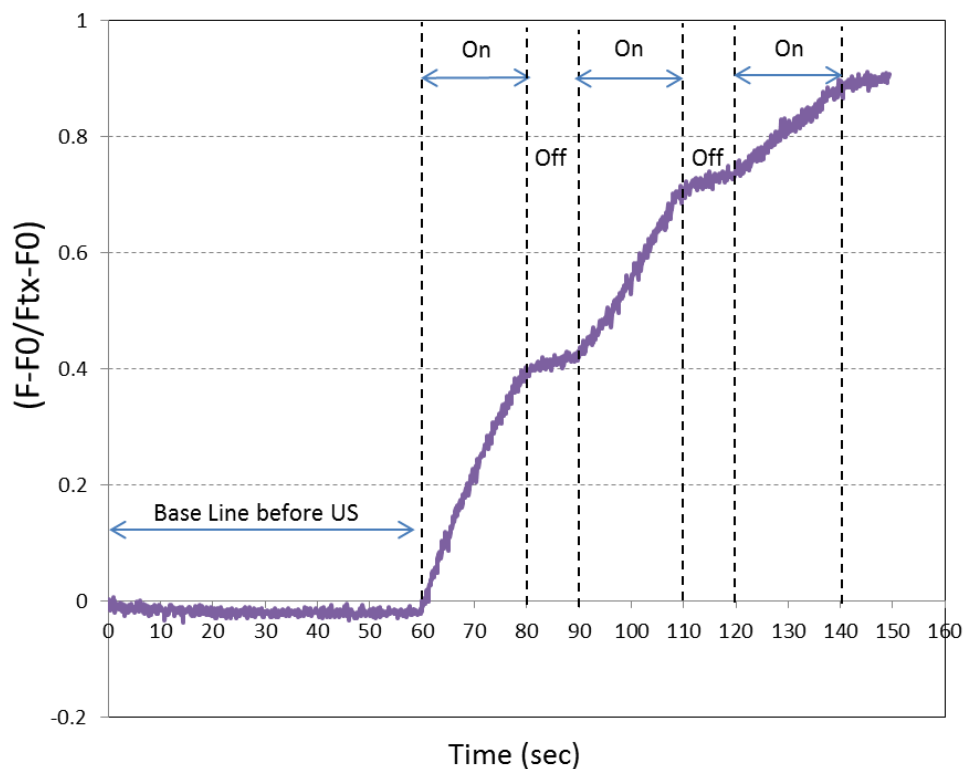


Figure 4.2: A typical normalized online LFUS release curve from targeted liposomes.

4.2.1. Online LFUS-induced release from DSPE-PEG-pNP control liposomes.

The graph in Figure 4.3 shows the release curves for the control liposomes at 20 kHz and the three different power densities mentioned previously. The light color zones around the lines are the error bars associated with the use of different liposome batches.

It can be observed that release was fast, reaching a stable value after 150 – 250s. The release rate increased with the increase in power density (see Fig. 4.4.A) and the final percentage of release was higher than 90% in all cases (see Fig. 4.4.B), meaning that the treatment with LFUS effectively released calcein from the liposomes.

The release data allowed for the calculation of an approximate initial release rate, determined as the calcein that was released after the second pulse of US (Figure. 4.4.A). Additionally, the final release was calculated by determining the maximum fluorescence attained after the liposomes were lysed by the addition of Tx100 (Figure. 4.4.B).

The statistical analysis of the results showed that the initial rate of release, measured as the percentage of fluorescence after the second 20s pulse of US, was significantly higher ($p = 1.10 \times 10^{-6}$) for a power density of 6.97 W/cm^2 ($61.67 \pm 6.93\%$)

than for the lowest power density of 6.08 W/cm² (47.23±6.95%). The rate of release at 11.83 W/cm² (68.64±5.39%) was also significantly higher ($p = 8.67 \times 10^{-3}$) than the one at 6.97 W/cm².

The comparison of the final percentages of release, on the contrary, showed no significant difference ($p = 0.25$) between 6.08 W/cm² (93.19±3.06%) and 6.97 W/cm² (95.36±3.16%). Also no statistical significant difference ($p = 0.47$) between 6.08 and 11.83 W/cm² (94.55±3.12%), and no significant difference ($p = 0.14$) between 6.97 and 11.83 W/cm² were observed.

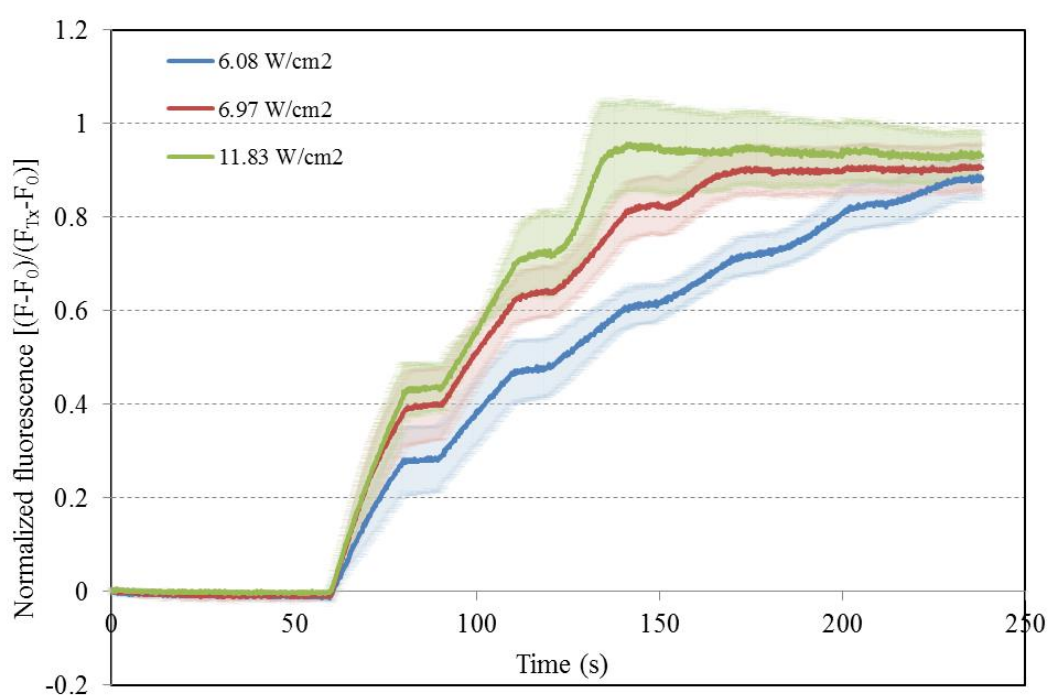


Figure 4.3: Calcein release curves from DSPE-PEG-pNP control liposomes, triggered by 20-kHz pulsed US (20 s on 10 s off) at different power densities. Results are average ± standard deviation of different liposome batches for each power density. The shaded areas are the error bars.

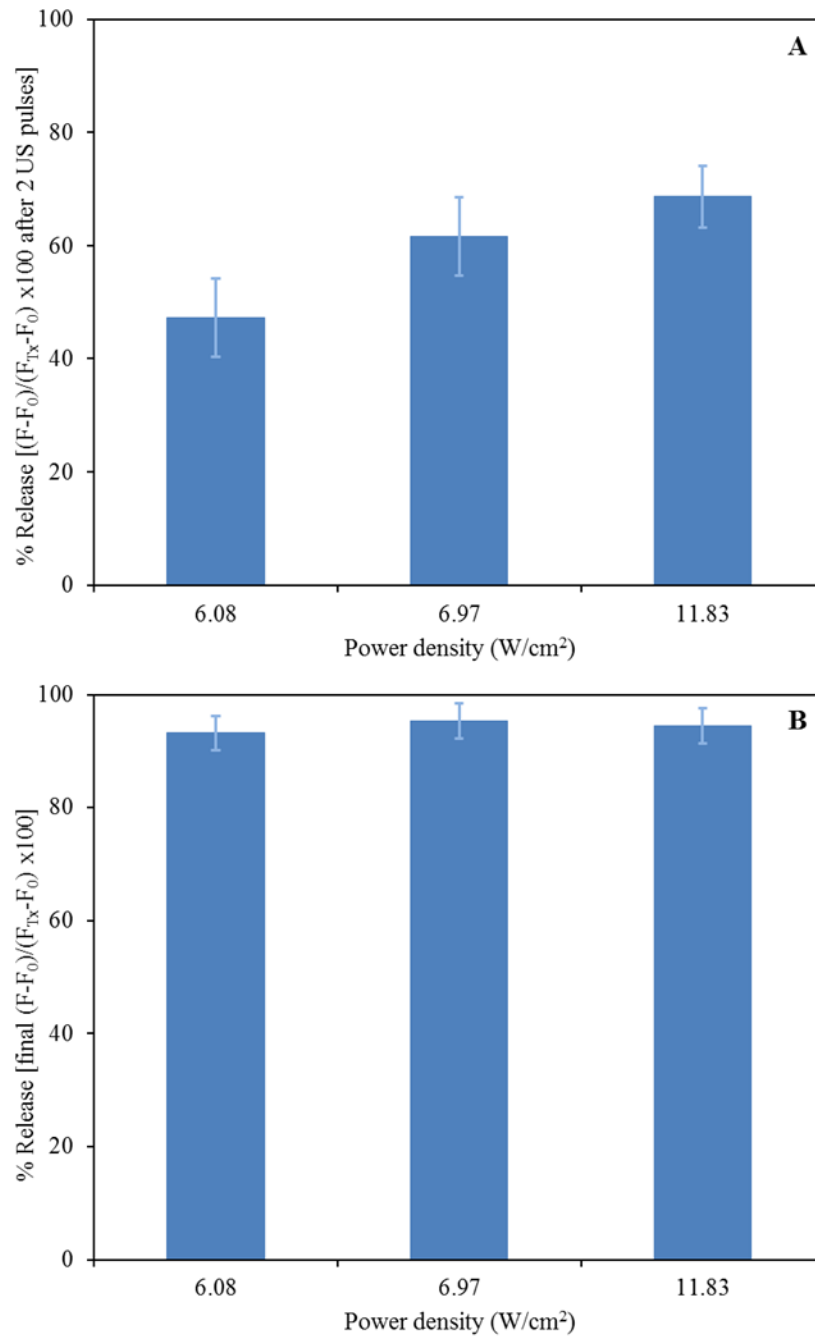


Figure 4.4: Comparison of the initial release rates of calcein (A) and final release percentage (B) from control DSPE-PEG-pNP liposomes at different power densities.

High release levels are expected using PEGylated liposomes. It was observed that increasing the PEG composition of the liposomes up to 5 mol% increased the US-triggered release [71]. In addition, DSPE-containing liposomes are expected to have high release levels.

A comparison between two different liposomes, (DPPC-cholesterol-[DOPE-PEG-pNP] and DPPC-cholesterol-[DSPE-PEG-pNP]) can be reported here. The former type was studied previously by our research group [69]. Both types of liposomes contain DPPC but differ in the lipid type connected to PEG and in the amount of lipids used in the synthesis. It was observed that DOPE-containing liposomes had a much slower release rate profile: maximum release was attained at around 10 minutes insonation, compared to 2.5 minutes for DSPE-containing liposomes. In addition, DOPE liposomes final release of calcein was less than 90% even at the highest power density, while DSPE liposomes had a final released above 90% even at the lowest power density. The different release profiles and rates may be explained by the differences in the molecular structures of DOPE and DSPE. Unsaturated lipids, such as DOPE, have *cis* bonds which decrease the ability of lipids packing and its transition temperature ($-16\text{ }^{\circ}\text{C}$), whereas DSPE lipids are saturated and can pack easily causing a high transition temperature ($74\text{ }^{\circ}\text{C}$) [72]. As a result, their leakage levels are different [71]. Because DSPE lipids have high transition temperature, they are more rigid behaving as a solid-like material. When triggered by US, the DSPE-containing liposomes will “break” open, while the DOPE-containing liposomes which have lower transition temperature, behave as gel-like material at the release temperature, releasing slower. Hence, DOPE-containing liposomes exposed to US are expected to release slower than DSPE-containing liposomes at the same power density and frequency (same attenuation and temperature).

4.2.2. Online LFUS-induced release from DSPE-PEG-Albumin liposomes.

The graph in Figure 4.5 shows the release curves for the albumin-targeted liposomes at 20 kHz, with the three different power densities mentioned previously. The light color zones around the lines are the error bars associated with the use of different liposome batches.

Similar to the release observed of the control liposomes, the release is fast, reaching a stable value after 150 – 250s. Also in this case, the release rate increases with increasing power density (Figure. 4.6.A) and the final percentage of release is higher than 90% for all power densities investigated (Figure.4.6.B).

The statistical analysis of the results showed that the initial rate of release (the percentage of fluorescence after the second 20 s pulse of US) was significantly lower ($p = 8.79 \times 10^{-6}$) for a power density of 6.08 W/cm^2 ($35.57 \pm 1.78\%$), when compared to 6.97

W/cm² (52.83±6.26%) and also significantly lower ($p = 1.08 \times 10^{-6}$) than the one obtained at 11.83 W/cm² (56.87±5.00%). The initial rate of release at 11.83 W/cm² (56.87±5.00%) was not significantly different ($p = 0.07$) from the one at 6.97 W/cm², unlike of the release observed from control liposomes.

The comparison of the final percentages of release showed no significant difference ($p = 0.66$) between 6.08 W/cm² (90.63±7.88%) and 6.97 W/cm² (91.94±2.77%). Also no significant difference ($p = 0.61$) between 6.08 and 11.83 W/cm² (95.86±1.49%), and no significant difference ($p = 0.79$) between the 6.97 and 11.83 W/cm² power densities were observed.

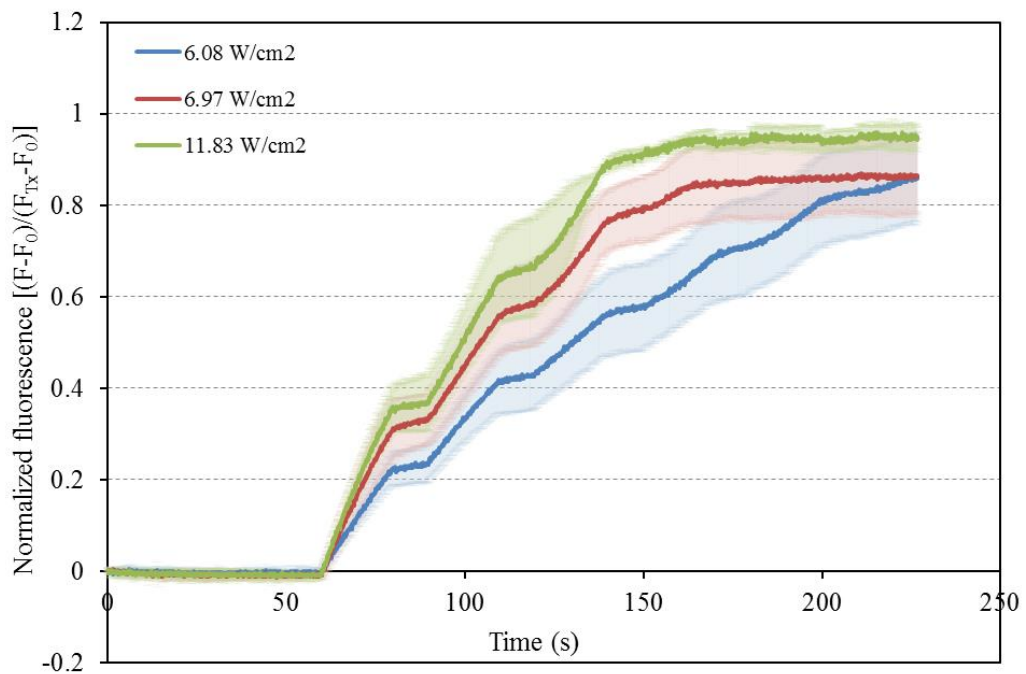


Figure 4.5: Calcein release curves from DSPE-PEG-albumin liposomes, triggered by 20-kHz pulsed US (20 s on 10 s off) at different power densities. Results are average \pm standard deviation of different liposome batches for each power density. The shaded areas are the error bars.

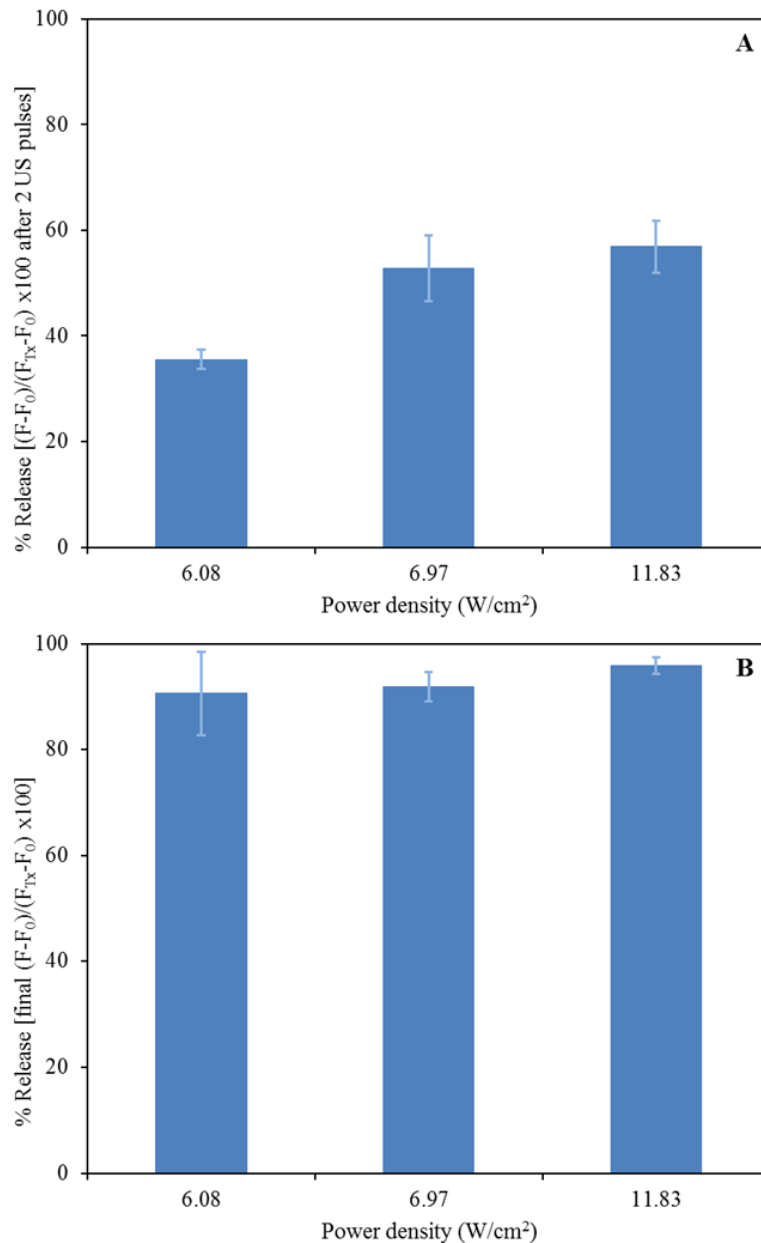


Figure 4.6: Comparison of the initial release rates of calcein (A) and final release percentage (B) from DSPE-PEG-albumin liposomes at different power densities.

4.2.3. Comparison between US release from targeted micelles and targeted liposomes.

While no acoustically activated release from targeted liposomes has been previously reported, acoustic power has been employed to trigger the release of chemotherapeutics from folated (folic acid targeted) micelles [73, 74]. Initial drug release percentages from these targeted micelles were higher, in part because their structure is composed of a single layer, as opposed to the phospholipid bilayer comprising the liposomes [75]. Two seconds were sufficient to cause approximately 8%

release of Dox from Pluronic® P105 micelles at 6 W/cm², using low-frequency ultrasound [76]. While the micellar studies reported earlier and the liposomal study reported in this thesis were not performed in identical conditions (70- vs. 20-kHz ultrasound, Dox vs. calcein, folic acid vs. albumin), a comparison is still worthwhile here because both frequencies are in the LFUS range, and both encapsulated chemicals have similar structures and molecular weights.

4.2.4. Comparison between control and Albumin-targeted liposomes.

Comparisons between initial release rates and final percentages of release were also performed for control *versus* albumin liposomes, for each power density. Figure 4.7 shows the comparison of the release curves for each power density.

To compare the release from targeted and non-targeted liposomes, two parameters were used: (i) the release rate, evaluated by the fluorescence after the second US pulse (Figure 4.8.A); (ii) the final release (Figure 4.8.B), as described previously.

Results show that, for the same US power density, the release from control liposomes is significantly faster than for the albumin liposomes (Figure 4.8.A) ($p = 6.40 \times 10^{-3}$ for 6.08 W/cm², $p = 9.51 \times 10^{-4}$ for 6.97 W/cm², and $p = 4.24 \times 10^{-4}$ for 11.83 W/cm²). A comparison of the final release from targeted and non-targeted liposomes (Figure 4.8.B), shows no significant differences at 6.08 W/cm² ($p = 0.36$) and at 11.83 W/cm² ($p = 0.59$), while the final release at 6.97 W/cm² is significantly higher ($p = 1.68 \times 10^{-2}$) for control liposomes. Hence, results suggest that the conjugation of the albumin moiety to the surface of the liposomes changes their acoustic properties, apparently increasing their stability and making them less susceptible to US.

Alternatively, since albumin is considered a natural nanocarrier (it can carry paclitaxel, as described in 2.1.5), it is possible that some albumin moieties, attached to PEG, capture some of the released calcein, hence decreasing its concentration in the solution, thus decreasing the fluorescence level. As a result, the apparent release rate of albumin liposomes will be lower than that from control PEGylated-only liposomes.

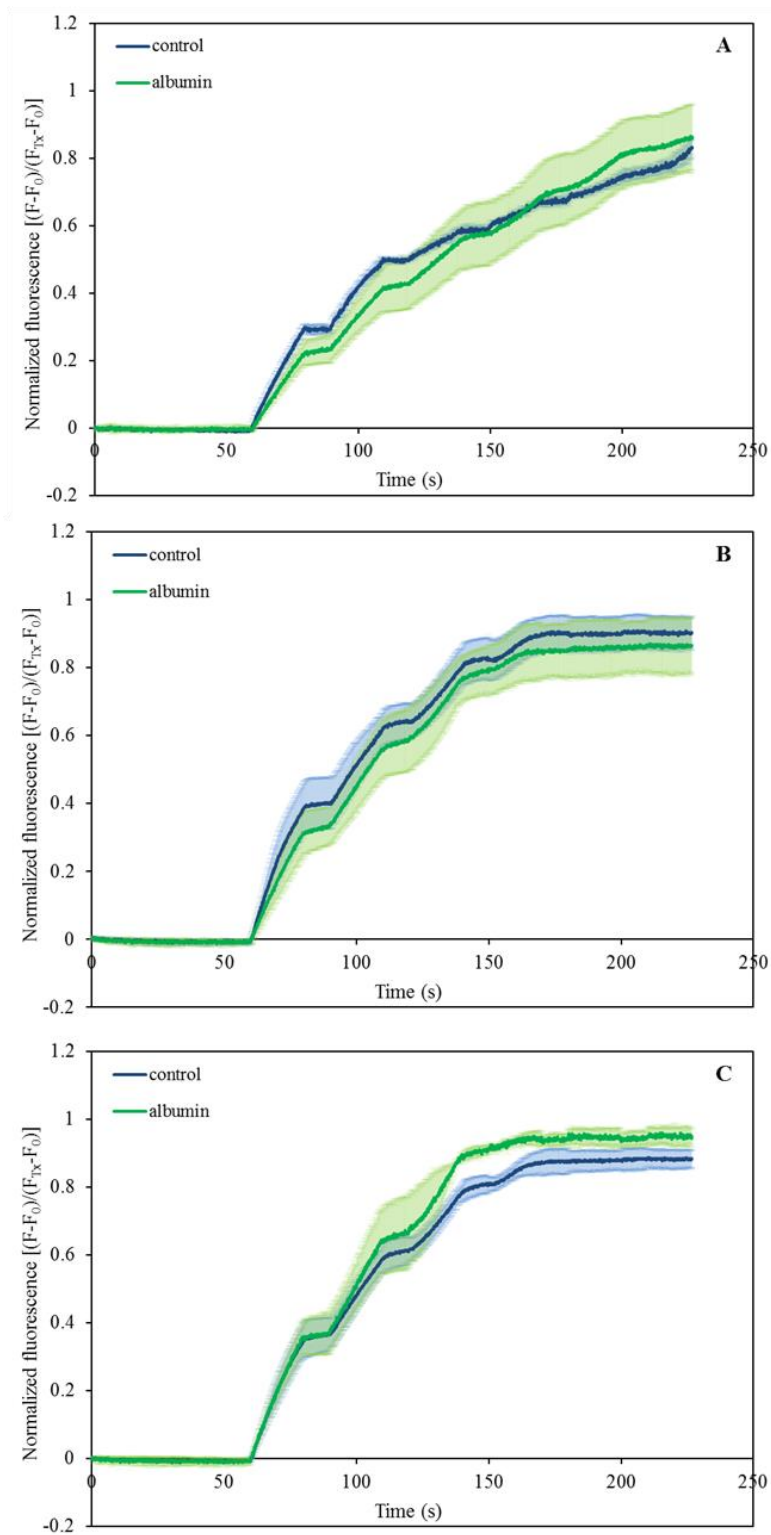


Figure 4.7: Comparison of the release curves for control and albumin liposomes at (A) 6.08 W/cm², (B) 6.97 W/cm², and (C) 11.83 W/cm². Results are average \pm standard deviation for 3 different liposome batches. The shaded areas are the error bars.

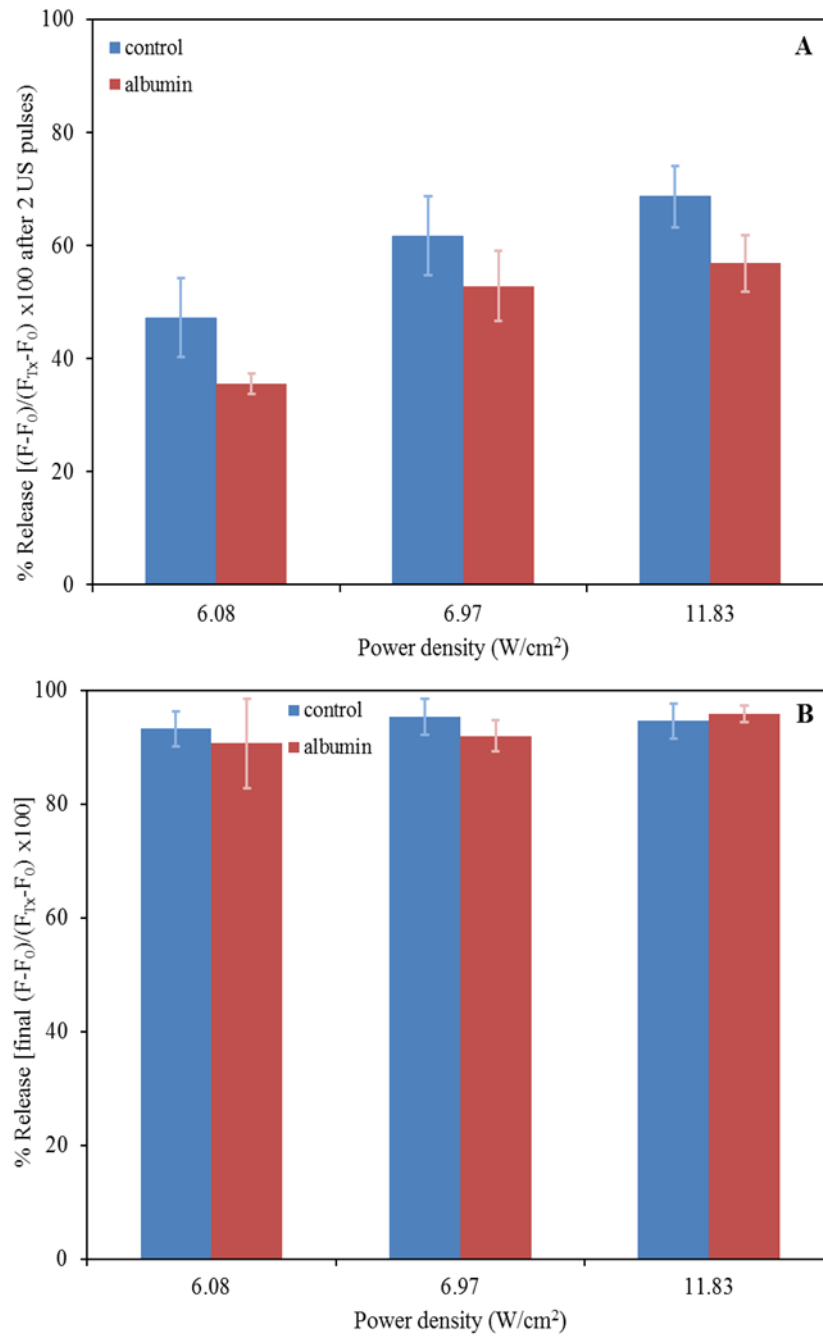


Figure 4.8: Comparison of the rates of calcein release from control and DSPE-PEG-albumin liposomes at different power densities. (A) after the second pulse of ultrasound; (B) final release.

In both cases, the calcein release is mainly caused by the mechanical effects (cavitation) of US. As the US frequency decreases, the threshold for transient cavitation decreases. Thus, at 20 kHz, using the 25 mm sonication probe, the mechanical index MI was calculated as 3.02, 3.23, 4.21 for 6.08, 6.97, 11.83 w/cm² power densities, respectively. The mentioned values of MI indicate that the cavitation is transient because

all values are above the transient threshold which is about 0.7 [77]. As a result of the bubble collapse, intense local heating, shock wave, micro streaming, and shear forces are produced [78]. Local heating causes hot spots with very high temperatures and pressures [79]. Such hyperthermia increases the permeability of the liposomal lipid layer, hence increasing the calcein release.

Chapter 5: Conclusion and Recommendations

Drug delivery systems, using nanoparticles as carriers for chemotherapy in cancer treatment, have been the interest of many scientists due to their huge advantage in reducing the adverse side effects, most importantly cardiac dysfunction. Liposomes are nanoparticles that have many advantages over other nanoparticles. They can encapsulate the drug and can travel to the cancer site with less clearance by the immune system, since their structure resembles that of cells. Once they reach the tumor site, they release their anti-neoplastic encapsulated content via three mechanisms: passive, active, and triggered targeting. Ultrasound has been widely studied as a trigger to release liposome-encapsulated drugs to the desired cells.

Two types of liposomes have been studied in this work: control liposomes (no moieties attached) and albumin-modified liposomes (proteoliposomes or albumin-targeted liposomes). The work presented in this thesis may be divided into two parts. First, several methods were utilized to prepare the liposomes until the best formulation was chosen. Control liposomes were prepared as DSPE-PEG-pNP liposomes, while albumin-modified liposomes were prepared from control liposomes, and then reacted with albumin under specified conditions to chemically attach the protein to their surface. Second, both types of liposomes were tested for their size by DLS, and calcein release triggered by LFUS. For both liposome types, the 20-kHz ultrasound-induced release reached a final stable value about 90% after 150 – 250 s for all power densities. The release rate increased with increasing power densities. The release from non-targeted liposomes was significantly faster than for albumin liposomes, at the same power density. The average diameters were determined to be 208.52 ± 11.50 nm for non-targeted control liposomes, and 218.27 ± 12.73 nm for albumin liposomes.

As a continuation of this work, it is recommended to study the release of such liposomes triggered with HFUS because it is the type of US used in medical imaging [70]. Furthermore, an *in vitro* study has to be performed to examine the interaction of targeted-liposomes with cancer cells overexpressing albumin receptors (e.g., prostate cancer cell line DU-145).

References

- [1] “What Is Cancer?,” *National Cancer Institute*, [Online]. Available: <http://www.cancer.gov/cancertopics/cancerlibrary/what-is-cancer>, 2014 [Accessed Oct. 20, 2015].
- [2] “Cancer Fact Sheet N°297,” *World Health Organization*, [Online]. Available: <http://www.who.int/mediacentre/factsheets/fs297/en/>, 2014 [Accessed Oct. 20, 2015].
- [3] P. Anand, A. B. Kunnumakkara, A. B. Kunnumakara, C. Sundaram, K. B. Harikumar, S. T. Tharakan, O. S. Lai, B. Sung, and B. B. Aggarwal, “Cancer is a preventable disease that requires major lifestyle changes.,” *Pharm. Res.*, vol. 25, no. 9, pp. 2097–116, Sep. 2008.
- [4] R. Siegel, D. Naishadham, and A. Jemal, “Cancer Statistics , 2012,” *CA. Cancer J. Clin.*, vol. 62, pp. 10–29, 2012.
- [5] J. Conde, J. M. de la Fuente, and P. V Baptista, “Nanomaterials for reversion of multidrug resistance in cancer: a new hope for an old idea?,” *Front. Pharmacol.*, vol. 4, no. October, p. 134, Jan. 2013.
- [6] P. Nygren, “What is cancer chemotherapy ?,” *Acta Oncol. (Madr).*, vol. 40, no. 3, pp. 166–174, 2001.
- [7] J.-J. Monsuez, J.-C. Charniot, N. Vignat, and J.-Y. Artigou, “Cardiac side-effects of cancer chemotherapy.,” *Int. J. Cardiol.*, vol. 144, no. 1, pp. 3–15, Sep. 2010.
- [8] D. T. Sugerman, “Chemotherapy,” *JAMA*, vol. 310, no. 2, p. 218, 2013.
- [9] “Chemotherapy,” Belvoir Media Group, LLC, Norwalk, Nov. 2010. Available: <http://ezproxy.aus.edu/login?url=http://search.proquest.com/docview/1370739922?accountid=16946>, [Accessed Oct. 25,2015].
- [10] “Cancer multidrug resistance,” *Nat. Biotechnol.*, vol. 18, pp. 18–20, 2000.
- [11] G. A. Hussein and W. G. Pitt, “Micelles and nanoparticles for ultrasonic drug and gene delivery.,” *Adv. Drug Deliv. Rev.*, vol. 60, no. 10, pp. 1137–52, Jun. 2008.
- [12] F. Alexis, E. M. Pridgen, R. Langer, and O. C. Farokhzad, “Drug Delivery,” vol. 197, M. Schäfer-Korting, Ed. Springer Berlin Heidelberg, 2010, pp. 55–86.
- [13] R. Singh and J. W. Lillard, “Nanoparticle-based targeted drug delivery.,” *Exp. Mol. Pathol.*, vol. 86, no. 3, pp. 215–23, Jun. 2009.
- [14] N. Nasongkla, E. Bey, J. Ren, H. Ai, C. Khemtong, J. S. Guthi, S. Chin, A. D. Sherry, D. A. Boothman, and J. Gao, “Multifunctional Polymeric Micelles as Cancer-Targeted, MRI-Ultrasensitive Drug Delivery Systems,” *Nano Lett.*, vol. 6, no. 11, pp. 2427–2430, 2006.
- [15] V. Torchilin, “Multifunctional and Stimuli-Sensitive Pharmaceutical Nanocarriers.,” *Eur J Pharm Biopharm*, vol. 71, no. 3, pp. 431–441, 2009.
- [16] M. R. Mozafari, a Pardakhty, S. Azarmi, J. a Jazayeri, a Nokhodchi, and a Omri, “Role of nanocarrier systems in cancer nanotherapy.,” *J. Liposome Res.*, vol. 19, no. 4, pp. 310–321, 2009.
- [17] G. A. Hussein and W. G. Pitt, “The Use of Ultrasound and Micelles in Cancer Treatment,” *J. Nanosci. Nanotechnol.*, vol. 8, no. 5, pp. 2205–2215, May 2008.

- [18] W. G. Pitt, G. A. Hussein, B. L. Roeder, D. J. Dickinson, D. R. Warden, J. M. Hartley, and P. W. Jones, "Preliminary Results of Combining Low Frequency Low Intensity Ultrasound and Liposomal Drug Delivery to Treat Tumors in Rats," *J. Nanosci. Nanotechnol.*, vol. 11, no. 3, pp. 1866–1870, Mar. 2011.
- [19] A. Schroeder, J. Kost, and Y. Barenholz, "Ultrasound, liposomes, and drug delivery: principles for using ultrasound to control the release of drugs from liposomes.," *Chem. Phys. Lipids*, vol. 162, no. 1–2, pp. 1–16, Nov. 2009.
- [20] J. Wu and W. L. Nyborg, "Ultrasound, cavitation bubbles and their interaction with cells.," *Adv. Drug Deliv. Rev.*, vol. 60, no. 10, pp. 1103–16, Jun. 2008.
- [21] U. A. R. Duane O. Hall, Sandy and C. Selfridge, Los Gatos, "Multi-frequency ultrasound therapy systems and methods," U.S. Patent 5460595, 1995.
- [22] G. P. Mishra, M. Bagui, V. Tamboli, and A. K. Mitra, "Recent applications of liposomes in ophthalmic drug delivery.," *J. Drug Deliv.*, vol. 2011, p. 863734, Jan. 2011.
- [23] A. Gabizon, D. C. Price, J. Huberty, R. S. Bresalier, and D. Papahadjopoulos, "Effect of Liposome Composition and Other Factors on the Targeting of Liposomes to Experimental Tumors : Biodistribution and Imaging Studies1," *Cancer Res.*, vol. 50, pp. 6371–6379, 1990.
- [24] K. Lee, K. Hong, and D. Papahadjopoulos, "Recognition of liposomes by cells: In vitro binding and endocytosis mediated by specific lipid headgroups and surface charge density," *Biochim. Biophys. Acta - Biomembr.*, vol. 1103, no. 2, pp. 185–197, Jan. 1992.
- [25] C. Kirby and G. Gregoriadis, "The effect of the cholesterol content of small unilamellar liposomes on the fate of their lipid components," *Life Sci.*, vol. 27, no. 23, pp. 2223–2230, Dec. 1980.
- [26] V. P. Torchilin, "Passive and Active Drug Targeting: Drug Delivery to Tumors as an Example" in *Drug Delivery*, vol. 197. M. Schafer-Korting, Ed. Boston: Springer Berlin Heidelberg, Nov. 2010, pp. 3-53.
- [27] P. S. Low and R. J. Lee, "Folate-mediated tumor cell targeting of liposome-entrapped doxorubicin in vitro," *Biochim. Biophys. Acta*, vol. 1233, pp. 134–144, 1995.
- [28] A. Kolate, D. Baradia, S. Patil, I. Vhora, G. Kore, and A. Misra, "PEG - A versatile conjugating ligand for drugs and drug delivery systems.," *J. Control. Release*, vol. 192C, pp. 67–81, Oct. 2014.
- [29] M. L. Immordino and L. Cattel, "Stealth liposomes : review of the basic science , rationale , and clinical applications , existing and potential," *Int. J. Nanomedicine*, vol. 1, no. 3, pp. 297–315, 2006.
- [30] W. G. Pitt, G. A. Hussein, and L. N. Kherbeck, "Ultrasound-triggered Release from Micelles," in *Smart Materials for Drug Delivery*, vol. 1, no. 2, C. Lorenzo and A. Concheiro, Eds. The Royal City of Chemistry, 2013, pp. 148–178.
- [31] H. Maeda, "The enhanced permeability and retention (EPR) effect in tumor vasculature: the key role of tumor-selective macromolecular drug targeting," *Adv. Enzyme Regul.*, vol. 41, no. 1, pp. 189–207, May 2001.
- [32] Q. Lin, G. Jiang, and K. Tong, "Dendrimers in Drug-Delivery Applications," *Des. Monomers Polym.*, vol. 13, no. 4, pp. 301–324, Jun. 2010.
- [33] K. Madaan, S. Kumar, N. Poonia, V. Lather, and D. Pandita, "Dendrimers in drug delivery and targeting: Drug-dendrimer interactions and toxicity issues.," *J. Pharm. Bioallied Sci.*, vol. 6, no. 3, pp. 139–50, Jul. 2014.

- [34] C. Lovelyn and A. Attama, "Current State of Nanoemulsions in Drug Delivery," *J. Biomater. Nanobiotechnol.*, vol. 2, no. 5, pp. 626–639, 2011.
- [35] J. Lattin, W. G. Pitt, D. Belnap, and G. A. Hussein, "Ultrasound-induced Cancein Release From eLiposomes," *Ultrasound Med. Biol.*, vol. 38, no. 12, pp. 2163–2173, 2012.
- [36] M. J. Hawkins, P. Soon-Shiong, and N. Desai, "Protein nanoparticles as drug carriers in clinical medicine.," *Adv. Drug Deliv. Rev.*, vol. 60, no. 8, pp. 876–85, 2008.
- [37] C. Obasaju and G. Hudes, "Paclitaxel and docetaxel in prostate cancer.," *Hematol Oncol Clin North Am*, vol. 15, no. 3, pp. 525–545, 2001.
- [38] S. Jang, M. Wientjes, D. Lu, and J. Au, "Drug delivery and transport to solid tumors," *Pharm. Res.*, vol. 20, no. 6, pp. 1337–1350, 2003.
- [39] A. K. Iyer, G. Khaled, J. Fang, and H. Maeda, "Exploiting the enhanced permeability and retention effect for tumor targeting.," *Drug Discov. Today*, vol. 11, no. 17–18, pp. 812–880, Sep. 2006.
- [40] B. Theek, F. Gremse, S. Kunjachan, S. Fokong, R. Pola, M. Pechar, R. Deckers, G. Storm, J. Ehling, F. Kiessling, and T. Lammers, "Characterizing EPR-mediated passive drug targeting using contrast-enhanced functional ultrasound imaging.," *J. Control. Release*, vol. 182, pp. 83–89, May 2014.
- [41] A. A. Gabizon, "Pegylated Liposomal Doxorubicin : Metamorphosis of an Old Drug into a New Form of Chemotherapy," *Cancer Invest.*, vol. 19, no. 4, pp. 424–436, 2001.
- [42] T. Lammers, F. Kiessling, W. E. Hennink, and G. Storm, "Drug targeting to tumors: principles, pitfalls and (pre-) clinical progress.," *J. Control. Release*, vol. 161, no. 2, pp. 175–187, Jul. 2012.
- [43] V. P. Torchilin, "Strategies and Means for Drug Targeting: An Overview," in *Biomedical Aspects of Drug Targeting*, V. Muzykantov and V. Torchilin, Eds. Springer New York, 2002, pp. 3–26.
- [44] J. T. Busher, "Serum Albumin and Globulin," in *Clinical Methods: The History, Physical, and Laboratory Examinations*, 3rd ed., H. J. Walker HK, Hall WD, Ed. Boston, 1990, pp. 497 – 499.
- [45] S. Dreis, F. Rothweiler, M. Michaelis, J. Cinatl, J. Kreuter, and K. Langer, "Preparation, characterisation and maintenance of drug efficacy of doxorubicin-loaded human serum albumin (HSA) nanoparticles.," *Int. J. Pharm.*, vol. 341, no. 1–2, pp. 207–214, Aug. 2007.
- [46] C. Vuarchey, S. Kumar, and R. Schwendener, "Albumin coated liposomes: a novel platform for macrophage specific drug delivery," *Nanotechnol. Dev.*, vol. 1, no. 1, Jul. 2011.
- [47] W. G. Pitt, G. A. Hussein, and B. J. Staples, "Ultrasonic drug delivery--a general review.," *Expert Opin. Drug Deliv.*, vol. 1, no. 1, pp. 37–56, Nov. 2004.
- [48] D. O. Draper, J. C. Castel, and D. Castel, "Rate of temperature increase in human muscle during 1 MHz and 3 MHz continuous ultrasound.," *J. Orthop. Sports Phys. Ther.*, vol. 22, no. 4, pp. 142–50, Oct. 1995.
- [49] P. E. Huber, J. W. Jenne, R. Rastert, I. Simiantonakis, H. Sinn, H. Strittmatter, D. Von Fournier, M. F. Wannemacher, and J. Debus, "A New Noninvasive Approach in Breast Cancer Therapy Using Magnetic Resonance Imaging-guided Focused Ultrasound Surgery," *Cancer Res.*, vol. 61, pp. 8441–8447, 2001.
- [50] V. Singh and M. Shrivastava, "Ultrasonic Hyperthermia for Cancer Treatment,"

- Natl. Phys. Lab.*, vol. 43, no. 3, pp. 235–241, 1993.
- [51] W. C. Dewey, “Arrhenius relationships from the molecule and cell to the clinic.,” *Int. J. Hyperthermia*, vol. 25, no. 1, pp. 3–20, Feb. 2009.
- [52] N. Rapoport, Z. Gao, and A. Kennedy, “Multifunctional nanoparticles for combining ultrasonic tumor imaging and targeted chemotherapy.,” *J. Natl. Cancer Inst.*, vol. 99, no. 14, pp. 1095–1106, Jul. 2007.
- [53] G. A. Husseini and W. G. Pitt, “Ultrasonic-Activated Micellar Drug Delivery for Cancer Treatment,” *J. Pharm. Sci.*, vol. 9999, no. 9999, pp. 795–811, 2008.
- [54] V. Frenkel, “Ultrasound mediated delivery of drugs and genes to solid tumors.,” *Adv. Drug Deliv. Rev.*, vol. 60, no. 10, pp. 1193–208, Jun. 2008.
- [55] K. W. Ferrara, “Driving delivery vehicles with ultrasound.,” *Adv. Drug Deliv. Rev.*, vol. 60, no. 10, pp. 1097–1102, Jun. 2008.
- [56] A. Azagury, L. Khoury, G. Enden, and J. Kost, “Ultrasound mediated transdermal drug delivery.,” *Adv. Drug Deliv. Rev.*, vol. 72, pp. 127–43, Jun. 2014.
- [57] S. B. Stringham, M. A. Viskovska, E. S. Richardson, S. Ohmine, G. A. Husseini, B. K. Murray, and W. G. Pitt, “Over-Pressure Suppresses Ultrasonic-Induced Drug Uptake,” *Ultrasound Med. Biol.*, vol. 35, no. 3, pp. 409–415, Dec. 2014.
- [58] R. Silva, H. Ferreira, C. Little, and A. Cavaco-Paulo, “Effect of ultrasound parameters for unilamellar liposome preparation.,” *Ultrason. Sonochem.*, vol. 17, no. 3, pp. 628–632, Mar. 2010.
- [59] S. Huang and R. C. MacDonald, “Acoustically active liposomes for drug encapsulation and ultrasound-triggered release.,” *Biochim. Biophys. Acta*, vol. 1665, no. 1–2, pp. 134–141, Oct. 2004.
- [60] B. M. Gabizon AA1, Barenholz Y, “Prolongation of the circulation time of doxorubicin encapsulated in liposomes containing a polyethylene glycol-derivatized phospholipid: pharmacokinetic studies in rodents and dogs.,” *Pharm. Res.*, vol. 10, no. 5, pp. 703–708, 1993.
- [61] M. Hsu and J. RL, “Interactions of liposomes with the reticuloendothelial system. II: Nonspecific and receptor-mediated uptake of liposomes by mouse peritoneal macrophages.,” *Biochim. Biophys. Acta*, vol. 720, no. 4, pp. 411–419, Sep. 1982.
- [62] K. Furumoto, J.-I. Yokoe, K. Ogawara, S. Amano, M. Takaguchi, K. Higaki, T. Kai, and T. Kimura, “Effect of coupling of albumin onto surface of PEG liposome on its in vivo disposition.,” *Int. J. Pharm.*, vol. 329, no. 1–2, pp. 110–116, Feb. 2007.
- [63] J. Yokoe, S. Sakuragi, K. Yamamoto, T. Teragaki, K. Ogawara, K. Higaki, N. Katayama, T. Kai, M. Sato, and T. Kimura, “Albumin-conjugated PEG liposome enhances tumor distribution of liposomal doxorubicin in rats.,” *Int. J. Pharm.*, vol. 353, no. 1–2, pp. 28–34, Apr. 2008.
- [64] E. L. Yuh, S. G. Shulman, S. A. Mehta, J. Xie, L. Chen, V. Frenkel, M. D. Bednarski, and K. C. P. Li, “Delivery of Systemic Chemotherapeutic Agent to Tumors by Using Focused Ultrasound : Study in a Murine Model 1,” *Radiology*, vol. 234, pp. 431–437, 2005.
- [65] V. P. Torchilin, “p -Nitrophenylcarbonyl-PEG-PE-liposomes : fast and simple attachment of specific ligands , including monoclonal antibodies , to distal ends of PEG chains via p -nitrophenylcarbonyl groups,” *Biochim. Biophys. Acta*, vol. 1511, pp. 397–411, 2001.
- [66] H. Grüll and S. Langereis, “Hyperthermia-triggered drug delivery from temperature-sensitive liposomes using MRI-guided high intensity focused

- ultrasound,” *J. Control. Release*, vol. 161, no. 2, pp. 317–327, Jul. 2012.
- [67] “Bicinchoninic Acid Protein Assay Kit,” Sigma-Aldrich, Missouri, USA, Rep., 2012.
- [68] “How DLS works.” [Online]. Available: <http://wyatt.eu/index.php?id=how-dls-works>, [Accessed January. 10, 2016].
- [69] S. Ahmed, “Dynamics of Chemotherapeutic Drug Release from Liposome Using Low-Frequency Ultrasound,” M.S. Thesis, Chemical Eng. Dept., American University of Sharjah., UAE, 2015.
- [70] S. L. Huang, “Liposomes in ultrasonic drug and gene delivery,” *Adv. Drug Deliv. Rev.*, vol. 60, no. 10, pp. 1167–1176, Jul. 2008.
- [71] M. Pong, S. Umchid, A. J. Guarino, P. A. Lewin, J. Litniewski, A. Nowicki, and S. P. Wrenn, “In vitro ultrasound-mediated leakage from phospholipid vesicles,” *Ultrasonics*, vol. 45, pp. 133–145, 2006.
- [72] B. Moghaddam, S. E. McNeil, Q. Zheng, A. R. Mohammed, and Y. Perrie, “Exploring the correlation between lipid packaging in lipoplexes and their transfection efficacy,” *Pharmaceutics*, vol. 3, no. 4, pp. 848–864, 2011.
- [73] G. A. Hussein, G. D. Myrup, W. G. Pitt, D. a Christensen, and N. Y. Rapoport, “Factors affecting acoustically triggered release of drugs from polymeric micelles,” *J. Control. Release*, vol. 69, no. 1, pp. 43–52, 2000.
- [74] G. A. Hussein, M. A. Diaz de la Rosa, E. S. Richardson, D. A. Christensen, and W. G. Pitt, “The role of cavitation in acoustically activated drug delivery,” *J. Control. Release*, vol. 107, no. 2, pp. 253–261, 2005.
- [75] G. A. Hussein, D. Velluto, L. Kherbeck, W. G. Pitt, J. A. Hubbell, and D. A. Christensen, “Investigating the acoustic release of doxorubicin from targeted micelles Ghaleb,” *Colloids and Surfaces B: Biointerfaces*, vol. 101, pp. 153–155, 2013.
- [76] G. A. Hussein, L. Kherbeck, W. G. Pitt, J. A. Hubbell, D. A. Christensen, and D. Velluto, “Kinetics of Ultrasonic Drug Delivery from Targeted Micelles,” *J. Nanosci. Nanotechnol.*, vol. 15, no. 3, pp. 2099–2104, 2015.
- [77] R. E. Apfel and C. K. Holland, “Gauging the likelihood of cavitation from short-pulse, low-duty cycle diagnostic ultrasound,” *Ultrasound Med. Biol.*, vol. 17, no. 2, pp. 179–185, Jan. 1991.
- [78] M. Margulis, *Sonochemistry and Cavitation*. Amsterdam: Gordon and Breach Science Publishers, 1995, p. 543.
- [79] K. S. Suslick, “Sonoluminescence and sonochemistry,” in *Ultrasonics Symposium, 1997. Proceedings., 1997 IEEE*, vol. 1, pp.523-532, 5-8 Oct. 1997.

Vita

Renad Zuhair Turki was born on May 02, 1991, in Amman, Jordan. She moved to the UAE in 1998 where she received her primary, elementary, and secondary education. She graduated, with distinction, from Al Rashid Al Saleh Private School in 2009. She received a merit Scholarship to the American University of Sharjah, from which she graduated as a *cum laude*, in 2013. Her degree was a Bachelor of Science in Chemical Engineering.

In 2013, Ms. Turki received a graduate assistantship and started her M.S. program in Chemical Engineering at the American University of Sharjah. She worked as teaching, laboratory, and research assistant for two years at the same university.